NUCLEON SPIN STRUCTURE STUDIES WITH POLARIZED PROTON AND ANTIPROTON BEAMS

N. Akchurin[5], M. E. Beddo[1], N. I. Belikov[4], A. Bravar[5,16], G. Burleson[11], J. Bystricky[2], M. D. Corcoran[15], A. A. Derevschikov[4], H. Enyo[6], R. Giacomich[16], M. Giorgi[16], D. A. Grachov[4], D. P. Grosnick[1], D. A. Hill[1], K. Imai[6], K. Kuroda[9], G. S. Kyle[11], J. L. Langland[5], F. Lehar[2], A. de Lesquen[2], D. Lopiano[1], D. Magauda[10], T. Maki[12], A. Masaike[6], Yu. A. Matulenko[4], A. P. Meschanin[4], J. McPherson[5], S. Mukhopadhyay[11], S. B. Nurushev[4], F. Olchowski[5], Y. Onel[5], D. I. Patalakha[4], A. Penzo[16], G. F. Rappazzo[10], M. Rawool-Sullivan[11], J. B. Roberts[15], A. Ruggeri[10], V. L. Rykov[4], G. Salvato[10], P. Schiavon[16], J. Skeens[15], J. Soffer[3], V. L. Solovyanov[4], L. F. Soloviev[4], H. Spinka[1], R. Takashima[7], F. Takeutchi[8], N. Tamura[13], D. G. Underwood[1], A. N. Vasiliev[4], A. Yokosawa[1], T. Yoshida[14] and A. Zanetti[16]

[1] Argonne National Laboratory, Argonne, Illinois, USA
[2] Centre d'Etudes Nucleaires, Saclay, France
[3] Centre de Physique Théorique, CNRS, Marseille, France
[4] Institute of High Energy Physics, Serpukhov, Russian Federation
[5] Department of Physics, University of Iowa, Iowa City, Iowa, USA
[6] Kyoto University, Kyoto, Japan
[7] Kyoto University of Education, Kyoto, Japan
[8] Kyoto-Sangyo University, Kyoto, Japan
[9] Laboratoire d'Annecy de Physique des Particules, Annecy, France
[10] University of Messina and INFN Messina, Messina, Italy
[11] Department of Physics, New Mexico State University, New Mexico, USA
[12] University of Occupational and Environmental Health, Kita-Kyushu, Japan
[13] Okayama University, Okayama, Japan
[14] Osaka City University, Osaka, Japan
[15] T. W. Bonner Nuclear Laboratory, Rice University, Houston, Texas, USA
[16] University of Trieste and INFN Trieste, Trieste, Italy

August 31, 1992

spokesman : A. Penzo
(Penzo@VAXTS)
deputy spokesman : Y. Onel
(Onel@IOWA)
contact person : A. Bravar
(Bravar@FNAL)

Abstract

A second generation of polarization experiments at Fermilab, aimed at significantly expanding the first-round E704 programme on high energy spin effects, can provide novel information on the problem of the proton spin composition, which is at present subject to an intense debate.

Contents

1 Introduction

Results on polarized muon deep inelastic scattering [1] suggest that the overall contribution of constituent quarks to the proton helicity is small, thus implying an appreciable contribution either of sea (strange) quarks, or of gluons or possibly of orbital angular momentum to the proton spin structure [2].

The subject, which is at present very actively investigated, both theoretically and experimentally, has deep implications for our view of the nucleon structure and of the QCD framework [3].

While a number of experiments using polarized lepton beams [4] are presently in progress or in preparation at various laboratories, in order to check and extend these results, the use of polarized beams of protons (antiprotons), interacting with polarized or unpolarized proton and nuclear targets, gives a uniquely distinct opportunity for performing a study of the nucleon spin structure with hadronic probes.

Over the last few years, the Fermilab E704 collaboration has been developing a rather complete setup for spin physics, based on the MP beam line of polarized protons/antiprotons [5], a target system with both LH_2 and polarized protons and an experimental apparatus composed of a magnetic spectrometer and electromagnetic calorimeters.

During the 1990 fixed target run, first round measurements were performed simultaneously both with the forward spectrometer and the large angle electromagnetic calorimeter, providing a number of new results on the x_F and the x_T dependence of transverse spin asymmetry in the inclusive production of charged and neutral pions and Λ particles.

These results suggest on one side the existence of spin dependent selection rules in the recombination processes of constituent quarks at large x_F, and a possible precocious onset of a hard regime at $x_F \approx 0$, as indicated by x_T scaling in the appearance of large asymmetries [6].

A number of theoretical ideas has been triggered by these results emphasizing the role of transverse single spin effects both in terms of higher twist effects, internal orbital angular momentum or soft-hard interaction interference effects [7].

During part of the 1990 run also the polarized proton target was successfully used for measurements of helicity dependent total cross sections and (parasitically) for double spin effects in production of neutral pions.

In conclusion, all parts of the MP facility have been operating very satisfactorily, comprising:

- the 100-200 GeV/c $p/\bar{p}$ polarized beam ($\langle P \rangle \approx 45\%$), with rapid polarization reversal (*snake*), instantaneous polarization tagging, and polarimeter systems;
- the frozen spin polarized target;
- the experimental setup with complete coverage of the forward CM hemisphere: the x_F and x_T useful regions are not acceptance limited, but depend only on statistics.

At present this fully operational Fermilab facility is unique and the potential of high energy spin physics has been reviewed in recent workshops [8]; possible improvements of the MP beam line for upgrading the maximum energy and the intensity have been discussed, as well as the impact of accelerating polarized beams of protons, in the framework of the Main Injector project [9] by using the Siberian Snake concept, which has been recently demonstrated with success in a series of experiments at IUCF [10]. This option is being actively studied [11] and could become one of the novel high-quality features of fixed target physics at Fermilab in the Main Injector era.

On basic physics grounds, much attention has been focussed on the mentioned problem of nucleon spin composition, which is currently referred to as the *spin crisis* in quantum chromodynamics; two approaches to this problem are developing. The first approach is based on perturbative QCD mechanisms in which the gluons give the main contribution to the proton spin. In the second one [12] this effect is explained by the nonperturbative structure of the QCD vacuum which leads to a strong polarization of sea quarks.

These two mechanisms differ by the characteristic scale of distances between quarks in the proton at which the main contributions appear. In the first case small distances (with typical transverse momenta of the quarks $k > m_p$) dominate, while in the second one the effect is important at large distances between quarks (and $k \approx 0$). Several realistic tests of the various suggested mechanisms for complementing the too small overall contribution of valence quarks, have been outlined [2, 3].

In particular it has been pointed out that the production of prompt photons or charmonium would be suitable for studying the gluon helicity in a polarized proton [13].

The optimal conditions for these experiments would certainly take advantage of beam upgrades in the MP line, and largely profit by the possible availability of high intensity accelerated polarized beams.

According to recent recommendations of PAC, we are considering this last option versus the former one, by realistically estimating the relative figure of merit (in statistical accuracy, running time, flux and rate limitations, costs, etc.), according to the specific implications for the measurements to be performed.

Measurements that have been suggested [2, 3] besides the two above - mentioned, have different types of requirements, sometimes not only related to beam intensity; for the ones discussed in this proposal, consideration to this aspect will be given when appropriate, in order to displicit the relative advantages of both cases.

We feel that the MP polarized facility has a specific potential for a second round of measurements aimed at clarifying the *spin crisis* dilemma, taking advantage of the presently available intensities and experimental setup, quite suitable for such studies.

- For instance, the investigation of the helicity composition of the proton can be initiated already by studying, with the polarized MP beamline, spin correlation parameters in processes involving final hyperons: reactions of this type have been discussed already some time ago [14] as efficient analyzers of the polarization of strange quarks or gluons in a polarized proton.

- The availability of polarized antiprotons in the MP beamline is an additional and unique feature, that can be exploited when trying to single out the contributions of valence quarks, with respect to gluon or sea constituents.

- One of the most useful tools in the investigation of the space-time characteristics of different process mechanisms are the nuclear targets. The nuclear medium can effectively act as a filter for hard-perturbative and soft-nonperturbative quark processes [15].

This last possibility is related with the concept of color transparency that was applied also to the large spin effects in the elastic polarized *pp* scattering.

In this proposal we discuss a series of measurements that could be done using the present configuration of the MP beam line and apparatus, in order to obtain expeditiously significant results that are relevant, in a new and complementary way (with respect to the deep inelastic scattering experiments), to the spin structure of the nucleon.

In a broader perspective, such timely experimental activity would also provide a foundation for participating to a robust program with high-intensity polarized proton beams from the Main Injector, by obtaining in advance physics information on subjects that are logically propaedeutic to the next stage, carrying over the expertise accumulated in the field of polarization experiments by our collaboration. For the time being the polarized antiproton beam is a unique option of the MP beam-line, and we feel that it should be exploited fully.

Some of the questions we would like to address directly are:

- the relative importance of (transverse) spin or helicity for the polarization dynamics of hadronic processes,
- the role of various parton species (valence quarks, sea quarks, gluons) in the spin composition of nucleons,
- the space-time scale of different mechanisms responsible for large spin asymmetries, in connection with colour transparency breaking in nuclei.

2 Basic QCD asymmetries

Contrary to single (transverse) spin effects, that are difficult to accomodate in the perturbative QCD framework, double helicity asymmetries in processes produced by interactions of longitudinally polarized beams and targets, can be obtained in the parton model from calculations involving the polarized constituent distributions and the elementary asymmetries corresponding to perturbative QCD diagrams.

Therefore it should be possible, for selected processes in appropriate kinematical regions, to test the helicity dependence of QCD, using the polarized structure functions measured in deep inelastic scattering, and alternatively

to evaluate, in the framework of perturbative QCD, the helicity distributions of constituents that are not directly accessible in deep inelastic scattering.

For example, it is important to have the experimental ability of measuring the helicity of gluons in a polarized proton directly. This is possible by studying with polarized beam and target the basic subprocesses (Fig.1), in the kinematical region where they dominate:

a) $gg \longrightarrow q\bar{q}$

b) $gq \longrightarrow q\gamma$

For these processes the helicity asymmetry:

$$A_{LL}^{ii} = \frac{\sigma(+,+) - \sigma(+,-)}{\sigma(+,+) + \sigma(+,-)}$$

is related to the basic constituent asymmetry $\hat{a}_{LL}^{ii}$:

$$A_{LL}^{ii} = \frac{\sum \int \Delta F_A^a(x_a, Q^2)\, \Delta F_B^b(x_b, Q^2)\, R_C^c(x_c, Q^2)\, \hat{a}_{LL}^{ii}\, d\sigma}{\sum \int F_A^a(x_a, Q^2)\, F_B^b(x_b, Q^2)\, R_C^c(x_c, Q^2)\, d\sigma}$$

where the functions $F_{A,B}(x, Q^2)$ give the probability for a hadron A or B to fragment into constituents a or b, with fractional momentum x, and R represents the probability for a parton c to recombine to a hadron C, carrying a fraction x of its momentum; the functions $\Delta F = [F(+,+) - F(+,-)]$ give the helicity distribution of a parton type in a hadron, and in first order QCD, $\hat{a}_{LL}^{ii}$ is given in Fig.2.

Therefore, for example in process a) $(gg \rightarrow q\bar{q})$ $\hat{a}_{LL}^{ii} \approx -1$ and

$$A_{LL}^{ii} \approx \left\langle \frac{\Delta G}{G}(x_1) \right\rangle \left\langle \frac{\Delta G}{G}(x_2) \right\rangle \hat{a}_{LL}^{ii} \approx -\left(\left\langle \frac{\Delta G}{G}(x) \right\rangle \right)^2$$

where G is the gluon structure function.

For processes like prompt photon and charmonium production, corresponding to the diagrams in Fig.1, the relationship to QCD is clear, and they are well suited for studying the gluon polarization [13]; nevertheless they might be considered experimentally delicate and limited in statistics, as in the former case the simple structure at the photon vertex is paid for by the small coupling constant, and in the latter case the high mass of the

$c\bar{c}$), which sets the scale for perturbative theory to apply, corresponds also to limited production rates.

It should be pointed out, however, that already during the previous E-704 run, clean signals have been obtained parasitically both for the production of prompt photons and of J/Psi, thus indicating that the factor influencing the quality of the results, that could be obtained in these channels is statistical accuracy and not experimental ability.

For production of light quarks, for instance in meson production, it would be more complicate to isolate in a clear way one definite diagram and therefore for these processes the effect of gluon polarization can be diluted and the information more difficult to extract.

However, first results on A_{LL}^{ii} from E-704 in π^0 production both with protons and antiprotons, compared with a QCD-based, hard scattering model, tend to indicate that the fraction of the proton spin carried by gluons is negligible (Fig.3). It would be important to push this comparison further, by increasing the statistical precision and the p_T coverage of the data, also to exploit the proton and antiproton results simultaneously to discriminate processes associated with interacting valence quarks or gluons.

In the same spirit the measurement of the asymmetry in the production of kaons and Λ hyperons with longitudinally polarized beam and target has a specific interest both because of the specific signature given by producing another flavour and the distinct negative sign of the basic asymmetry for the QCD diagrams involved (type E in Fig.2).

3 Hyperon processes

Since the first results on hyperon polarization at Fermilab [17], in particular for Λ, the origin of this polarization is discussed in terms of polarized s quarks, as the u and d couple in a singlet state, but the dynamical mechanisms for obtaining highly polarized $s\bar{s}$ pairs are still to be fully understood.

Recently a relatively simple and quite predictive model [18], gives a fair description both of the cross section and the polarization, which was not always the case for some previous fragmentation and recombination models [19]. Another dynamical model [20] leads to a quantitative description of the cross section via triple Regge exchange and of the polarization via interference of final states in processes of virtual dissociation into hyperon states $\Lambda, \Sigma, \Sigma^*$.

Also spin correlation parameters, which are calculable within these models, can be compared with new data obtained by us. For illustration we show in Fig.4 and Fig.5 the polarization, asymmetry and the depolarization parameters which were obtained in recent measurements with transversally polarized proton beam on liquid hydrogen target.

The production of strangeness via process $gg \rightarrow s\bar{s}$ should give rise to significant asymmetries both for polarized beam on polarized target, A_{LL}^{ii} as mentioned before, but also, due to the polarization self - analyzing properties of parity violating decays, to measurable correlations with the polarized beam. In this case the asymmetry is:

$$A_{LL}^{if} = \frac{\sum \int \Delta F_A^a(x_a, Q^2)\, F_B^b(x_b, Q^2)\, \Delta R_C^c(x_c, Q^2)\, \hat{a}_{LL}^{if}\, d\sigma}{\sum \int F_A^a(x_a, Q^2)\, F_B^b(x_b, Q^2)\, R_C^c(x_c, Q^2)\, d\sigma}$$

The first order perturbative QCD predictions for $\hat{a}_{LL}^{if}$ are given in Fig.6 and assuming full correlation between the s quark helicity and the Λ hyperon polarization:

$$A_{LL}^{if} \approx \left\langle \frac{\Delta G}{G} \right\rangle \hat{a}_{LL}^{if}$$

In Fig.7 are shown predictions [14] for both asymmetries.

For these predictions the polarized gluon structure functions are assumed to have a strong helicity dependence (Fig.8).

It should be noted that in both cases there is a significant dependence on the CM production angle, as a consequence of the helicity conserving nature of the underlying gluon interaction.

Gluon dominance in inclusive Λ production, which is expected to be valid when going to large energy and p_T, has still to be established experimentally.

4 Exploring the sea polarization

As previously discussed one of the alternative solutions to the ***spin crisis*** leads to a relatively large polarization of the sea in a polarized proton.

Part of the embarassment with the EMC result [1] is not only caused by the apparent contradiction with the ***naive*** idea of the spin of the proton being carried mainly by its constituent quarks, but even more by the failure of the Ellis-Jaffe sum rule (the counterpart for the proton of the Bjiorken sum rule,

relating the proton and neutron spin structure functions to the axial vector coupling, which is regarded as fundamental in QCD). The Ellis-Jaffe sum rule has been originally obtained in the hypothesis of negligible contribution from the strange sea quarks: in view of the experimental results, it seems important to test this hypothesis.

It has been suggested [21] that the study of the forward production of longitudinally polarized Λ hyperons by longitudinally polarized protons, could provide the possibility of measuring the helicity density of the strange quarks in the sea of a polarized proton. Using the MP-line longitudinally polarized proton and antiproton beams on a LH_2 target, this type of measurement would be feasible without modification of the present setup.

The EMC [1] result, combined with the axial vector coupling constants measured in the neutron and hyperon β decays, which are the ingredients of the Ellis-Jaffe sum rule, provides an estimate for the contributions of the u, d and s quarks, indicating that strange quarks carry a large fraction of the proton spin, namely

$$\Delta s = (s\uparrow + \bar{s}\uparrow) - (s\downarrow + \bar{s}\downarrow) = -0.24 \pm 0.07$$

This way the results can be reconciled with the Ellis-Jaffe sum rule (without neglecting the strange quark contribution), but still conflicting with the simple picture that the valence quarks build up the spin of the proton.

The possibility of a large and negative Δs is still subject to an intense debate, bearing also on the problem of the strangeness content of the nucleon [22], which is periodically claimed to be negligibly small or rather large, on the basis of reasons that seem in both cases quite respectable.

These arguments range from estimates of the pion-nucleon sigma-term which is a measure of chiral symmetry breaking, from π - N phase shift analysis which yield rather large values for $\langle p|s\bar{s}|p\rangle$ to the evaluation of the axial vector current matrix elements between nucleon states from elastic neutrino-proton scattering, where the initial analyses, leading to a small strangeness content, have been criticized [23] and again a large contribution from the strange sea advocated. From experiments on charm production from neutrinos, it can be deduced that, excluding the Pomeron contribution, diverging for small x, the strangeness content of the proton is rather small.

It has been demonstrated [24], on the basis of positivity, that the polarized strange quark distributions are bounded by the unpolarized one $s \geq \Delta s$ and

therefore any measurement aiming at obtaining information on Δs is also touching very sensitive areas, such as chiral symmetry breaking and OZI rule violation.

Results on a large and negative Δs might also suggest some more general interpretation. There is evidence recently reported by the NMC [25] that the Gottfried sum rule is violated and the simple interpretation is the existence of a flavour asymmetry in the light quark sea of the nucleon [26], namely $\bar{u}(x) \neq \bar{d}(x)$. In fact the data would require that $\bar{d}(x) \gg \bar{u}(x)$ and a way to understand this is, for example, to accept the idea that quarks are surrounded by a pion cloud so the excess of u quarks in the proton leads to an excess of $\pi^+(u\bar{d})$ over $\pi^-(\bar{u}d)$ [27].

The same picture with a kaon cloud around the quarks together with the fact that the transition $u \rightarrow s + K$ flips the quark helicity, leads to expect a large negative correlation between the helicity distributions Δu and Δs. As a result A_{LL}^{if} in inclusive Λ production is expected to be large and negative [21].

To be more specific in this picture, which is appealling as it connects the violation of spin (Ellis-Jaffe) and isospin (Gottfried) sum rules, the forward diffractive production can proceed via the exchange of a soft-nonperturbative Pomeron, which can directly couple to quarks via multiperipheral ladders.

In the Λ production the main subprocess at the top would correspond often to a certain class of fragmentation processes:

$$p \longrightarrow \Lambda + K \quad and \quad \bar{p} \longrightarrow \bar{\Lambda} + K$$

in the forward hemisphere (with large production cross section); the constituent valence u ($\bar{u}$) quark leaves the polarized p ($\bar{p}$) to form the forward kaon. In this picture the hyperon polarization arises from the averaged spin of the spectator ud system and the value Δs ($\Delta \bar{s}$) for the polarization of s ($\bar{s}$) quarks in the beam.

In the model of Ref. [18], it is assumed that the dominating subprocess at the end of the multiperipheral chain is $\pi + p \rightarrow K + \Lambda$, with the K on-shell and the pion only slightly off-shell. Then data from low energy experiments on the binary reaction $\pi + p \rightarrow K + \Lambda$ can be used to predict the high energy regime of the (semi-)inclusive Λ production.

It is worth noting that the pattern of Λ polarization for the exclusive reaction $pp \rightarrow \Lambda K^+ p$, has been measured at the ISR, and has been interpreted as evidence of pomeron-quark interaction.

In another approach to the relationship between flavour asymmetry of the sea light quarks, and their polarization [28], it was shown that the contribution of strange quarks is negligible but that the light quarks in the sea have asymmetrical distributions and contribute to the nucleon spin in such a way to reduce the value of the Ellis-Jaffe sum rule in agreement to the experimental result; the same percentual reduction would however also affect the Bjiorken sum rule. Improving our knowledge on the sea polarization for quarks and antiquarks is a very important challenge, if it appears that also this crucial sum rule might be violated [29].

There is no doubt about the feasibility of the experiments outlined here, with the E-704 apparatus in the MP line, in particular the diffractive Λ hyperon production, as the setup of the previous run can be integrally used; the acceptance is extending over the range (Fig.9):

$$0.2 \leq x_F \leq 0.8 \qquad 0.15 \leq p_T \leq 1.8\, GeV/c$$

Within this kinematical region a measurement of A_{LL}^{if} , would give thus an insight on the non - vanishing (strange) sea quark polarization; if this polarization is opposite to the proton helicity, such possible anticorrelation effect would be quite distinguishable from the effects of other competing mechanisms, which tend to produce positive correlations.

5 Estimation of A-dependence of one-spin asymmetries in meson production by polarized protons on nuclei

As noted above, perturbative QCD at large $p_\perp^2$ predicts A^1-dependence of inclusive cross sections on the basis of color transparency. Hence if the mechanism responsible for spin asymmetry A_N is described by perturbative QCD then A_N would not depend on the atomic number of the target nucleus due to fact that it corresponds to a ratio of cross sections having the same A-dependence. It means that in perturbative QCD we expect $A_N \sim A^\alpha$ with $\alpha \approx 0$ On the contrary if the mechanism includes large distances between quarks then it can lead to a large difference in the absorption of specific quark configurations in nuclei and to a sharp A-dependence of the asymmetries.

A nonperturbative model of the polarized proton wave function proposed recently in the papers [30] has been used here for the estimations of the nuclear effects. This model successfully describes the EMC experiment and other experimental data on the structure functions of sea quarks.

In this model an asymmetry in inclusive particle production appears due to the existence of asymmetric configurations in the hadron wave function $\Psi([x_i],[k_{\perp i}])$, caused by the quark interaction with the QCD vacuum fields (instantons) [31]; a similar mechanism has been proposed also in [32].

Inclusive meson spectra at large $x_F \to 1$, in this model result from two types of contributions:

$$\left(\frac{d\sigma}{dx_F}\right)_{pp\to\pi X} = \left(\frac{d\sigma}{dx_F}\right)^S + \left(\frac{d\sigma}{dx_F}\right)^{NS} =$$

$$C_1 \sum_i \int_{x_F}^1 \frac{dx}{x} q_{i/p}(x) G_{\pi/i}(x_F/x) +$$

$$+ C_2 \sum_n \int \prod_i [dx_i] \prod_i [dk_{\perp i}] \delta(x_F - x_1 - x_2) |\Psi_n([x_i],[k_{\perp i}])|^2$$

where C_1, C_2 are constants.

The first term is a perturbative QCD contribution, where $q_{i/p}(x)$ are the quark distribution function in the $k_{\perp i}$ symmetric configuration in the proton wave function. The second term describes the contribution of large distances in the cross section from the *internal* polarized nonperturbative sea [30]. Here $\Psi_n([x_i],[k_{\perp i}])$ is the n-particle Fock column component of the nucleon wave function.

According to this model for a polarized proton the dominant contribution comes from configurations with asymmetric distribution of quarks and antiquarks ($k_{i\perp} \gg k_{j\perp}$, $x_i \gg x_j$). This connects with the fact that for total angular momentum conservation in the spin-flips of valence quarks on nonperturbative fields a large orbital momentum transfer to the sea quarks is needed.

The basic contribution to the second term in the kinematical region $x_F \to 1$ $p_\perp^2 \geq 1 GeV^2$, where one-spin asymmetry in inclusive π-mesons production is observed [33], is the process of meson production from quark and antiquark with essentially different variables $x_1 \approx 0, x_2 \approx x_F; k_{\perp 1} \approx 0, k_{\perp 2} \geq 1 GeV$ in the five-quark component of the nucleon wave function $|N\rangle = |(3q)(\bar{q}q)\rangle$.

The asymmetry is obtained as follows:

$$A_N(x_F)|_{pp\to\pi X} = \frac{C_3 \cdot (d\sigma/dx_F)^{NS}}{(d\sigma/dx_F)^{S} + (d\sigma/dx_F)^{NS}}$$

$$A_N(x_F)|_{pA\to\pi X} = \frac{C_3 \cdot A_{eff}^{NS} \cdot (d\sigma/dx_F)^{NS}}{A_{eff}^{S} \cdot (d\sigma/dx_F)^{S} + A_{eff}^{NS} \cdot (d\sigma/dx_F)^{N_s}}$$

In the framework of the parton model in a nucleus only quite low partons with $x_i \approx 0$ can interact. Therefore for the symmetrical configuration with $(x_1 \approx x_2 \approx x_F/2)$ we expect an absence of nuclear absorption, i.e. *color transparency*. At the same time the asymmetric configuration with $x_1 \approx 0$, $x_2 \approx x_F$ must be absorbed with hadron cross sections. The nuclear factors are calculated by standard methods:

$$A_{eff}^{NS} = \int d^2b \cdot T(b) e^{-(\sigma_{pN}^{tot}+\sigma_{\pi N}^{tot})/2 \cdot T(b)}, \qquad A_{eff}^{S} \approx A^1$$

where $T(b) = A \cdot \exp(-b^2/R^2)/2\pi R^2$ is the nuclear profile function, which has been taken in the gaussian form.

In Fig.10(a,b) the calculation results of A-dependence asymmetries for $\pi^{\pm,0}$ meson production on nuclei Be, Al, Pb are shown together with our results for proton target. It can be concluded that if the mechanism of one-spin asymmetries connects with large nonperturbative effects then we should observe an A-dependence. On the contrary if the perturbative mechanism dominates, considerable nuclear effects are not expected and hence the asymmetry has to differ weakly from the proton one.

6 Experimental feasibility

A programme of measurements with the polarized proton (antiproton) beam and the E704 existing apparatus that we propose for the next fixed-target run can be sommarized as follows:

- Λ ($\bar{\Lambda}$) diffractive production with longitudinally polarized beams, over a range of (small) p_T values and (medium - large) x_F values; for these measurements with LH_2 target, the setup of the previous run can be used, with the advantage of being already fully tested for the detection and reconstruction of V^0.

- The same criteria apply to the measurements of π^{pm} on LH_2 and nuclear targets with transversally polarized beams. Additionally to the forward spectrometer, the small - angle and large angle electromagnetic calorimeters, can be used, as in the previous E704 run for the study of neutral pion production. For the measurements of Λ hyperon production, the E-M calorimeters will be also useful for tagging other hyperons (mainly Σ^0) as well as K_s^0 (that have already detected in the $\pi^0\ \pi^0$ channel with the E - M calorimeters). This is a definite extra bonus in using our multipurpose apparatus for more specific channels.

- For the investigation of the gluon helicity distribution in the production of strangeness via the process $gg \rightarrow s\bar{s}$ we should look for asymmetries both with longitudinally polarized beam and target, but also, for correlations of the helicities of the beam and of the produced Λ. As in both cases there is a significant dependence on the CM production angle, the region to be explored is defined by an interval:

$$0.25 \leq x_R \leq 0.50$$

with $x_R\ (= \sqrt{x_F^2 + x_T^2})$. This kinematical region can be suitably covered by the E704 forward spectrometer, with minor changes, in order to extend the acceptance to larger values of p_T and smaller values of x_F; rates for Λ production should be appreciable up to $p_T \approx 3\ GeV/c$.

The polarized target for the A_{LL}^{ii} measurements will consist of the same cryostatic system already used for E704, but loaded with ^6LiD with a high frequency (180 GHz) microwave source. The main merit of the ^6LiD target arises from the much smaller dilution factor of the polarization: in terms of running time required for a given accuracy on the asymmetry, the ^6LiD target represents a gain of about 14 over conventional target materials.

From the measurements performed in the previous fixed-target run, we have a complete understanding of the performance of our apparatus, both for the charged (pion) and for the neutral ($\pi^0 and \Lambda$) channels; for the Λ the overall distributions of x_F and p_T are given in Fig.9, showing that the kinematical region covered in E-704 is adequate for the first two types of measurements listed above. The experimental distributions of Fig.11 contain the effects of geometrical acceptance, trigger acceptance and reconstruction efficiency of our apparatus and therefore we have estimates for the data to

be collected, comprehensive of all these effects, including a number of losses connected realistic run conditions.

In order to evaluate the conditions for expanding the p_T coverage of the spectrometer, we have used the Monte Carlo programs developed for the setup and trigger studies for E-704, that have been later tuned on real data, for checking possible effects of reconstruction efficiency on the experimental distributions. With this programmes it is possible to generate events containing Λ particles, trace all the charged tracks through the spectrometer defining their hits on all the detectors, and feed these data to the same reconstuction program that was used for the analysis of the real data; it is also possible to generate minimum bias events to study the trigger rejection and to *implant* generated Λs onto real*background* events from the experimental tapes.

As it will be discussed later, the acceptance for Λ hyperons produced at the target and decaying to $p\pi^-$ from 1 m to 6 m downstream the target (more than 35 percent of such decays for Λs in the kinematical region of interest) was defined in the previous run by our trigger counters and not by the geometry of the apparatus.

From this study it turns out that it is quite simple to expand the coverage towards larger p_T by mainly extending the trigger counters and redefining the correlation patterns, with modest changes of the geometry of the spectrometer. The results of this study can be summarized in Fig.11, where the geometrical acceptance (a) and the reconstruction efficiency (b) are shown for the new configuration. This analysis shows that up to 3 GeV/c the geometrical acceptance is larger than 60 percent for $0.4 \leq x_F \leq 0.95$ and the reconstruction efficiency is larger than 40 percent. Concerning the trigger, a straightforward modification of the one used for the previous run would give very similar efficiency, close to 60 percent with rejection factors between 5 and 10, according to the kinematical region; however we are continuing the Monte Carlo studies, in order to adapt the trigger conditions to the requirements at larger p_T.

As the spin asymmetries are calculated from ratios of events, both acceptance (geometry and trigger) and efficiency (trigger and reconstruction) will drop out as the beam and target polarizations are frequently flipped. Therefore the knowledge of these parameters is more important for estimating correctly the achievable statistics and consequently the expected precision on the asymmetry, rather than for defining correction factors to the row rates

and distributions.

This is particularly true for single and double spin asymmetries; however in the case of spin correlation measurements, where the weak decay distribution of the Λ hyperons are used for extracting their polarizations, care has to be taken in preventing biassing these distributions. These effects have been studied already for our previous experiment, and a number of relevant considerations will be given in a subsequent section discussing the determination of the polarization asymmetries and spin transfer parameters.

7 Experimental setup

The apparatus, installed in the MP line, can be divided into four major components: the polarized beam, the target system, the forward spectrometer and the electromagnetic calorimeters.

7.1 The polarized beam

The polarized beam involves the production, transport, tagging and spin manipulation of the polarized protons; a complete description of the beamline (Fig.12) is published [5]. For both positively and negatively polarized tagged protons the averaged polarization is 45 percent; the tagging system has been confirmed by polarimeters based on Primakoff and CNI (Coulomb - Nuclear Interference) effects [34].

The final direction of the beam polarization is manipulated by a spin rotation system (*snake*) without disturbing the trajectory of the beam at the final focus (Fig.13). The spin can be changed from horizontal to vertical or longitudinal and can be reversed periodically, for suppressing systematic errors.

7.2 The target system

The target system allows alternate installation either of a 1 m long target, filled with liquid hydrogen, or of a polarized proton target (3 cm diameter, 20 cm long) [35], operating at a temperature of 0.4 K for obtaining the polarization build-up in a 2.5 T magnetic field with 70 GHz microwaves; once a polarization close to 0.7 is reached, the microwave is switched off,

and the temperature is decreased to less than 80 mK (frozen spin), in order to maintain the polarization for sufficient periods, even with low magnetic fields. For the ^6LiD target, polarization up to 0.7 is obtained at 5 T with 180 GHz microwave power [36]. In this case both p and n are polarized; the dilution factor is 0.5, to compare with 0.14 for conventional materials, the target density is 0.86 g/cm^3.

7.3 The forward spectrometer

The forward spectrometer stretches 50 meters from the target to the chamber farthest downstream, with its cross section approximate 1 meter high by 3 meters wide at the end. It is capable of recording a significant fraction of forward charged particle tracks coming out from the experimental target. Fig.14 shows all essential elements: 43 wire chamber planes and the 1.4 Tesla analyzing magnet (BM109) are responsible for the reconstruction of charged tracks angles/momenta.

Five hodoscope planes and a Cherenkov threshold counter act as a fast trigger system.

Three types of chambers are used in the spectrometer; most of the chambers are MWPC read-out with two types of electronics (RMH/PCOS3) with 2 mm wire spacing, the most critical ones at the beginning of the spectrometer have 1 mm wire spacing, at the end one drift chamber with sense wire spacing of approximately 19 mm. Most chamber modules have four plane views: X,Y,U,V with X and Y respectively horizontal and vertical and U and V symmetrically inclined by approximately 24 degrees from the the vertical axis.

Table I summarizes the setup of wire chambers, Table II contains informations on other detectors in the spectrometer.

The spectrometer has been working satisfactorily for beam fluxes of one million polarized protons per second (with efficiencies of each chamber better than 90 percent); higher fluxes can be tolerated if the beam area is desensitized with beam killers.

Λ hyperons, produced at the experimental target, decaying in a region downstream the target into proton and negative pion, can be detected by measuring their decay products in the chambers upstream the analyzing magnet, whose momentum could be determined using the downstream chamber telescope.

Events containing a candidate Λ decay are preferentially recorded, by selecting with the hodoscope setup configurations where a stiff track, corresponding to the proton in the asymmetric decay deflected by the analyzing magnet to beam-right into the Cherenkov counter acceptance, is accompanied by a softer track to beam-left, corresponding to the decay negative pion.

The acceptable configurations have been obtained from Monte Carlo studies and have been implemented in the trigger by means of PLU and MLU units (Fig.15). The selection criteria, as checked on real data in 1990, do not introduce appreciable biases on production or decay distribution of the accepted Λ.

The Cherenkov counter contains helium gas in a 1.5 meter diameter by 20 meters long cylindrical volume; photons emitted from charged particles traversing the counter volume are collected by four 50×50 cm mirror segments and focussed into single photoelectron sensitive phototubes. At a pressure of 4 psi, the threshold energy for pions is around 40 GeV/c; by using the Cherenkov signal to tag high energy pions, and taking advantage of the segmentation, events with positive pions faking the protons from Λ decay, are reduced.

Also the effect of this selection has been checked on real data, and found not to affect the reconstructed Λ distributions.

According to the arrival time of signals from various parts of the apparatus, stretching from the tagging station midway the beam line (200 m upstream the experimental target) to the most downstream hodoscope, the trigger is divided in three logical levels:

I geometrical/interaction level ($RIGHT \bullet LEFT \bullet INT$)

II proton arm and pion arm correlation level ($PROT \bullet PI$)

III proton-pion correlation level, strobed by beam ($PROT \bullet PI \bullet BEAM$)

The wire chambers are strobed with level I, and on occurrence of level III, the data are validated for storage on tape. Collection of the data was performed in 1990 by CAMAC interfaced PDP11/45 frontend computer, connected to a VAX-3100 workstation for online monitoring. The data taking rates were typically 1200 triggers/spill: a higher throughput ($>$ 5000 events/spill) can be obtained with an optimized acquisition system based on dedicated VME dual port fast memory buffers and MC68020 processors: the transfer rate can be in excess of 1 Mbyte/sec.

7.4 The Electromagnetic Calorimeters

Two sets of lead - glass counters are used for determining the energy and impact position of electromagnetic showers mainly produced by pairs of photons from neutral pion decays [37].

The central region around the beam is covered by an array of 125 lead glass counters ($6.35\ cm \times 6.35\ cm$) with a thickness of 13 X_0, placed at a distance of 50 m from the target.

At larger angles ($40\ -\ 140\ mrad$) two arrays of about 1000 counters each, are positioned symmetrically with respect to the beam axis at 10 m from the target. The energy resolution obtained in previous run is given by $dE/E = 0.05/\sqrt{E} + 0.02$.

8 Event reconstruction and selection

On the basis of the wire chamber information, charged tracks are reconstructed by the pattern recognition algorithm in the horizontal projections upstream and downstream of the analyzing magnet, as well as in the vertical projection across the whole spectrometer.

The magnet has a field integral of 3 Tm, appreciably uniform in the spectrometer acceptance, and the effect of minor components is negligible. The partial tracks are associated in three dimensions, using U,V coordinates, thus allowing momentum reconstruction for the individual trajectories.

The single track reconstruction efficiency is higher than 60 percent and for the subsequent selection of events containing a V^0 candidate, pairs of tracks are selected such that:

- the reconstructed decay vertex (from the closest approach of the two tracks in space upstream the magnet), is completely separate (downstream) from the target volume;
- the vector sum of momenta points to the production vertex and matches the beam impact point at the target,
- additionally we require also that the longitudinal momenta of the positive and negative tracks are asymmetrically distributed such that $\alpha = (p_L^+ - p_L^-)/(p_L^+ + p_L^-) > 0.5$ and the transverse components $q_T = q_T^+ = q_T^- < 0.15\ GeV/c$

these events lead to a clear Λ band in the $\alpha - q_T$ plane, corresponding to a very clean peak in invariant mass (Fig.16 and Fig.17), with small background from residual K_s^0 decays: most of these events are suppressed when using the Cherenkov counter in anticoincidence.

These conditions, optimized for selection of Λ (also for Σ^0), will be relaxed in order to accumulate simultaneously also consistent samples of K_s^0.

9 Determination of spin parameters

For the measurements we are interested in there are three types of asymmetries that can be obtained:

- The single spin asymmetry with transversally polarized beam is obtained by

$$A_N = \frac{1}{P_B} \frac{N(+) - N(-)}{N(+) + N(-)} \tag{1}$$

- The asymmetry with beam and target longitudinally polarized is obtained by

$$A_{LL}^{ii} = \frac{1}{P_B P_T} \frac{N(+,+) - N(+,-)}{N(+,+) + N(+,-)} \tag{2}$$

  from events with parallel $(+,+)$ and antiparallel $(+,-)$ beam - target polarization ($+/-$ refer to the beam/target helicity).

  To first order this asymmetry is independent from acceptance and detector efficiency bias, but it is affected by the large dilution factor of the target polarization.

- Measurements with polarized beam and unpolarized target allow for Λ hyperons to obtain

$$A_{LL}^{if} = \frac{2}{\alpha_\Lambda P_B} \frac{N(+,+) + N(-,-) - N(+,-) - N(-,+)}{N(+,+) + N(-,-) + N(+,-) + N(-,+)} \tag{3}$$

  from events with parallel $(+,+)$, $(-,-)$ and antiparallel $(+,-)$, $(-,+)$ beam and Λ polarization. enditemize

  The longitudianl Λ polarization can be extracted on the basis of the parity non - conserving decay distribution for the produced protons:

$$W_p = (1 + \alpha_\Lambda P_\Lambda cos\vartheta^*) \tag{4}$$

where P_B and P_Λ are the beam and ϑ^* is the C. M. angle of the decay proton.

Also in this case the relative acceptance and efficiency effects should cancel in the asymmetry in first order, however particular care has to be paid to the unambiguous discrimination of the most asymmetric (forward - backward) decay configurations, where the vertex reconstruction is quite delicate.

We have studied this problem by Monte Carlo simulation and it turns out that, by taking into account the correlation between the decay momentum asymmetry $(p - \pi)$ parameter α previously defined and the CM decay angle (Fig.18) it is possible to estimate the longitudinal component of the Λ polarization essentially free from vertex bias. This is substantially different from the same problem in the determination of the transverse Λ polarization and can be simply traced back to the fact that the forward-backward decay events are limited to the edges of the $cos\vartheta^*_L$ distribution while they affect a broader interval in the central region of the $cos\vartheta^*_N$ distribution; the subscript L and N refer respectively to the CM decay angles measured with respect to the Λ direction and to the normal to the production plane.

10 Rates and statistical accuracy

With the present spectrometer configuration the available x_F, x_T region is perfectly matched to studies at small transverse momentum, where statistics are very comfortable; this kinematical region is relevant to the study of possible contributions of strange sea to the proton helicity.

For these studies, a running time of 4 weeks would allow to collect approximately 400k events with a reconstructed Λ hyperon in the kinematical range

$$0.3 \leq x_F \leq 0.8 \qquad 0.10 \leq p_T \leq 1.0\ GeV/c$$

in order to achieve a $\delta A^{if}_{LL} = 0.03$ per bin.

For the studies at larger p_T, we can reduce the distance from target to magnet by 1/3 or move the magnet transversally by 0.5 m, in order

to increase the acceptance at larger p_T (both displacements are easily performed, as magnet and detectors are on rails).

Assuming a cross section at $p_T = 3GeV/c$, $x_F = 0.3$ of $6{\cdot}10^{-32}cm^2/GeV^2$, for 2400 hours of data taking with a ^6LiD polarized target ($\rho = 0.83\ g/cm^3, l = 20\ cm$) and $2 \cdot 10^7$ polarized proton beam/spill, we expect to obtain $2 \cdot 10^4$ Λ per bin ($0.5\ GeV/c$ at $p_T = 3\ GeV/c$). This would give an error in A_{LL}^{ii} of 0.04.

The accuracy achievable in this measurement depends crucially on the special merit of the ^6LiD material as a polarized target for inclusive reactions where the unpolarized nucleons in the target reduce the effective polarization P_T^{eff} with respect to that of the polarized protons ($P_T = 0.7 - 0.9$) by a factor that in standard materials can be as low as 0.15, while in ^6LiD,due to the high nuclear polarization, both for ^6Li and D, is only 0.5. We have assumed a running efficiency of 70 percent in the rate estimates.

11 Conclusions

We propose to exploit during the next fixed target Tevatron run the existing and fully debugged E704 setup on the MP polarized $p/\bar{p}$ beam line for performing the following measurements:

a) asymmetry A_N for charged and neutral pions (and K_s^0) produced by vertically polarized p ($\bar{p}$) on LH_2 and nuclear targets at medium p_T and over a wide range of x_F in order to study the relationship of colour transparency and spin dependence. No modification in the setup is required; the running time estimated for this measurement is 600 hours.

b) depolarization parameter A_{LL}^{if} at small p_T and medium x_F for Λ with longitudinally polarized p ($\bar{p}$) beams on LH_2 target, in order to explore the strange sea polarization. No modification in the setup is required; the running time for this measurements is estimated 800 hours.

c) depolarization parameter A_{LL}^{if} for Λ and Σ^0 hyperons over a range $0.25 < x_R < 0.5$ with longitudinally polarized proton beam on LH_2 target, in order to probe the gluon polarization. Minor modifications to the spectrometer have to be performed and running time is estimated 1200 hours.

d) Asymmetry A_{LL}^{ii} for Λ and Σ^0 hyperons, with longitudinally polarized proton beam and ${}^6LiD$ polarized target over a range $0.25 < x_R < 0.5$. Results also on asymmetry for pions and kaons could be obtained simultaneously during this run, in order to obtain a diversified set of data related to the contribution of gluons to the helicity composition of nucleons. The total required running time is 2400 hours.

In this case the major technical complications refer to the smooth running of the polarized target and to a multitrigger operation of the acquisition system. Both these aspects have been already taken care during the 1990 run of E704 with success.

Based on our experience during the previous run of fixed target physics, we are confident that, if scheduled during the next period for an overall

running time of approximately 7 months, we could achieve significant new results that would probe the role of spin for the structure and the dynamics of hadrons in a direct way.

Some of these experiments would not be necessarily easier at higher energies or with larger intensity and we feel that their requirements match ideally the MP polarized beam properties.

12 References

[1] J. Ashman et al. (EMC), Phys. Lett. **B206** (1988) 364
J. Ashman et al. (EMC), Nucl. Phys. **B238** (1989) 1
V.W. Hughes et al. (EMC), Phys. Lett. **B212** (1988) 511

[2] R.L. Jaffe and M. Manohar, Nucl. Phys. **B337** (1990) 509, and references therein

[3] G. Preparata and J. Soffer, Phys. Rev. Lett. **61** (1988) 1167
A.V. Efremov and O.V. Teryaev, *Dubna preprint* E-2-88-287 (1988)
S.J. Brodsky, J. Ellis and M. Karliner, Phys. Lett. **B206** (1988) 309
G. Altarelli and G.G. Ross, Phys. Lett. **B212** (1988) 391
R.D. Carlitz, J.C. Collins and A.H. Muller, Phys. Lett. **B214** (1988) 229

[4] NA47 at CERN: J. Cibrowski et al. (SMC), *Proposal* CERN/SPSC 88-47 (1988)
E142 at SLAC: R. Arnold et al., SLAC *Proposal* E142 (1989)
HERMES (HERA): K. Coulter er al., DESY/PRC 90-1 (1990)
HELP (LEP): G. Ballocchi et al., CERN/LEPC 89-10, LEPC/M88 (1989)

[5] D. Grosnick et al., Nucl. Inst. Meth. **A290** (1990) 269

[6] D.L. Adams et al., *High x_T single - spin asymmetry in π^0 and η production at $x_F = 0$ by 200 GeV/c polarized protons and antiprotons Preprint* FERMILAB-Pub-91/14-E (1991), to be published in Phys. Lett. B

[7] A.V. Efremov and O.V. Teryaev, Phys. Lett. **B150** (1985) 383, and reference therein
R.L. Jaffe and Xiangdong Ji, Phys. Rev. **D43** (1991) 724
D. Sivers, Phys. Rev. **D41** (1990) 83
J. Qiu and G. Sterman, Phys. Rev. Lett. **67** (1991) 2264

[8] See for instance:
Symp. on Future Polarization Physics at Fermilab, Fermilab 1988, Ed. E. Berger, J.G. Morfin. A.L. Read and A. Yokosawa
Int. Symp. on High Energy Spin Physics, Bonn 1990, Ed. K.H. Althoff and W. Meyer
Int. Workshop on Spin Phenomena in High Energy Physics, Protvino 1991
Adriatico Research Conference on Polarization Dynamics in Nuclear and Particle Physics, ICTP - Trieste Jan 1992, Ed. A.O. Barut, N. Paver, A. Penzo and R. Raczka

[9] D.G. Underwood et al., *Proc. Workshop on Physics at the Main Injector* (1989) 171, Ed. S.D. Holmes and B.D. Winstein

[10] A.D. Krisch et al., Phys. Rev. Lett. **63** (1989) 1137
J.E. Goodwin et al., Phys. Rev. Lett. **64** (1990) 2779

[11] A.D.Krisch et al., Spin effects in high- p_T^2 proton- proton elastic scattering, FNAL Proposal (Jan. 1992)

[12] S.Forte and E.V.Shuryak, Nucl.Phys. **B357** (1991) 153
A.E.Dorokov and N.I.Kochelev, Phys.Lett. **B259** (1991) 335

[13] E.L. Berger and J. Qiu, Phys. Rev. **D40** (1989) 778
J.L. Cortes and B. Pire, Phys. Rev. **D38** (1988) 3586
A.P. Contogouris et al., Phys. Lett. **B246** (1990) 523
M.A. Doncheski and R.W. Robinett, Phys. Lett. **B248** (1990) 188

[14] F. Baldracchini et al., Phys. Lett. **96B** (1980) 381
N.S. Craigie, K. Hidaka, M. Jacob and F.M. Renard, Phys. Reports, **99** (1983) 147

[15] S.J.Brodsky and A.H.Mueller, Phys.Lett. **206B** (1988) 685
J.P.Ralston and B.Pire, Phys.Rev.Lett. **65** (1990) 2343

[16] S.J.Brodsky and F. de Teramond, Phys.Rev.Lett. **60** (1988) 1924

[17] G. Bunce et al., Phys. Rev. Lett. **36** (1976) 1113
B. Lundberg et al., Phys. Rev. **D40** (1989) 3557
L.G. Pondrom, Phys. Reports **122** (1985) 57
K. Heller, *Proc.* 17^{th} *Int. Conf. on Polarization Phenomena in Nuclear Physics*, Paris 1990, Journal Phys. Coll. **51**, C6-163 (1990)

[18] J. Soffer and N.A. Törnqvist, Phys. Rev. Lett. **68** (1992) 907

[19] B. Anderson, G. Gustafson, G. Ingelman and T. Sjostrand, Phys. Reports **97** (1983) 31
T. DeGrand, J. Markkanen and H. Miettinen, Phys. Rev. **D32** (1985) 2445

[20] R. Barni, G. Preparata and P.G. Ratcliffe, Submitted to Phys. Rev. Lett.

[21] J. D. Bjorken has attracted our attention to these considerations; se also M. Karliner, *Proc. Symposium on Future Polarization Physics at Fermilab*, June 13 - 14 (1988) pag. 12

[22] R.Decker, M.Nowakowski and U.Wiedner, Strangeness in the nucleon, CERN Preprint CERN-PPE/92-010 (January 1992)

[23] D.B.Kaplan and A.Mahonar, Nucl.Phys. **B310** (1988) 1167

[24] G.Preparata and J.Soffer, Phys.Rev.Lett. **61** (1988) 1167

[25] P. Amaudruz et al. (NMC), Phys. Rev. Lett. **66** (1991) 2712

[26] G. Preparata, P.G. Ratcliffe and J. Soffer, Phys. Rev. Lett **66** (1991) 687

[27] J.D. Bjorken, *Preprint* SLAC-PUB-5608, July 1991

[28] F.Buccella and J.Soffer, CPT *Preprint*, Marseille, CPT-92/P 2706 (1992)

[29] E.J. Eichten, I. Hinchliffe and C. Quigg, *Preprint* FERMILAB-91/272-T LBL-31324

[30] A.E.Dorokhov and N.I.Kochelev Phys.Lett. **B259** (1991) 335
A.E.Dorokhov, N.I.Kochelev and Yu.A.Zubov. Argonne report PHY-7056-TH-92, JINR preprint E2-91-375 (1991) to be published in Int. Jorn. Mod. Phys

[31] N.I.Kochelev and M.V.Tokarev JINR Preprint E2-92-300 (1992)

[32] D.Sivers Phys.Rev. **D41** (1990) 83

[33] D.L.Adams et al. Phys. Lett. **B264** (1991) 462

[34] D.C. Carey et al., Phys. Rev. Lett. **64** (199) 357
N. Akchurin et al., Phys. Lett. **B229** (1989) 299

[35] P. Chaumette et al., *Advances in Cryogenic Eng.* 35 (1990), Ed. R.W. Fast, Plenum Press N.Y.

[36] P. Chaumette et al., *Proc. Symposium on High Energy Spin Physics*, Minneapolis, Minesota, Sept. 1988

[37] D.L. Adams et al., Phys. Lett. **B261** (1991) 201

[38] C. Nguyen, *Spin Effects in Inclusive* Λ *Production Using 200 GeV/c Polarized Protons*, Ph.D. Thesis, Rice University, Houston, Texas, June 1991

13 Figure Captions

Fig. 1: Two basic diagrams related to processes initiated by gluons, suitable for gluon helicity studies.

Fig. 2: The basic QCD asymmetry $\hat{a}_{LL}^{ii}$ for different classes of diagrams.

Fig. 3: A_{LL}^{ii} in π^0 production.

Fig. 4: P_0, A_N, $D_{NN}(= A_{NN}^{if})$ for $pp \rightarrow \Lambda X$ at 200 GeV/c versus x_F [38]. The dotted line in P_0 plot represents standard behaviour (for example Ref. [17]). A_N and D_{NN} data at 200 GeV/c are compared with K_s^0 and Σ^0 at 18.5 GeV/c.

Fig. 5: P_0, A_N, D_{NN} for $pp \rightarrow \Lambda X$ at 200 GeV/c versus p_F for all x_F (upper plots) and for $0.5 < x_F < 1.0$ (lower plots) [38]. See also Fig.10 for the p_T, x_F experimental distributions. The curves in the P_0 plots correspond to Ref. [18] (dashed line) and Ref. [20] (dash-dotted line) respectively for $x_F \approx 0.4$ (upper plot) and $x_F \approx 0.7$ (lower plot).

Fig. 6: The $\hat{a}_{LL}^{if}$ elementary asymmetry for processes $gg \rightarrow s\bar{s}$, $u\bar{u} \rightarrow s\bar{s}$.

Fig. 7: Predictions of [14] for helicity asymmetries in $pp \rightarrow \Lambda X$.

Fig. 8: $\frac{\Delta G}{G}$ for Ref. [14] and for recent models.

Fig. 9: The E704 experimental phase space for $pp \rightarrow \Lambda X$.

Fig. 10: E704 – A_N dependence on nuclei number.

Fig. 11: a) Gemetrical acceptance and b) Reconstruction efficiency for $pp \rightarrow \Lambda X$.

Fig. 12: The MP polarized beam line.

Fig. 13: The spin rotation system (*snake*) for obtaining any polarization component and for periodic reversal against systematic errors.

Fig. 14: The layout of the forward spectrometer of E704.

Fig. 15: The correlation maps of hodoscopes for selecting Λ *configurations*.

Fig. 16: The selected Λ invariant mass distribution.

Fig. 17: The V^0 decay phase space α q_T.

Fig. 18: The correlation between α and π or γ decay angles.

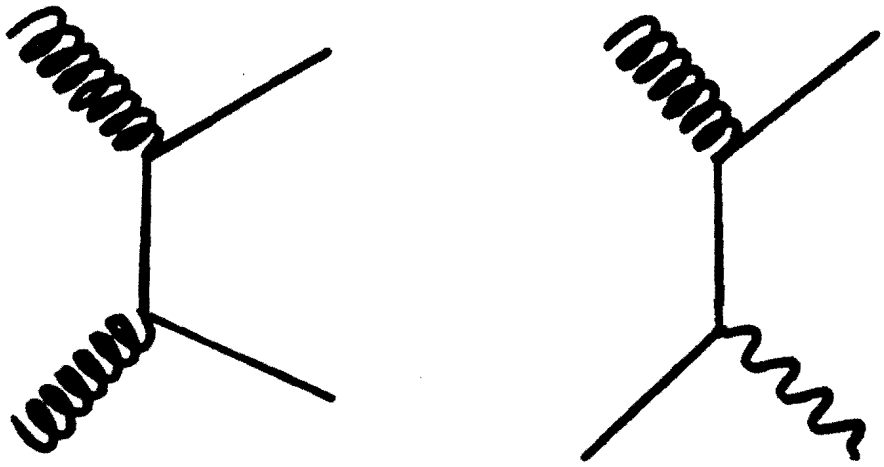

a) $gg \longrightarrow q\bar{q}$ b) $gq \longrightarrow q\gamma$

Fig. 1: Two basic diagrams related to processes initiated by gluons, suitable for gluon helicity studies.

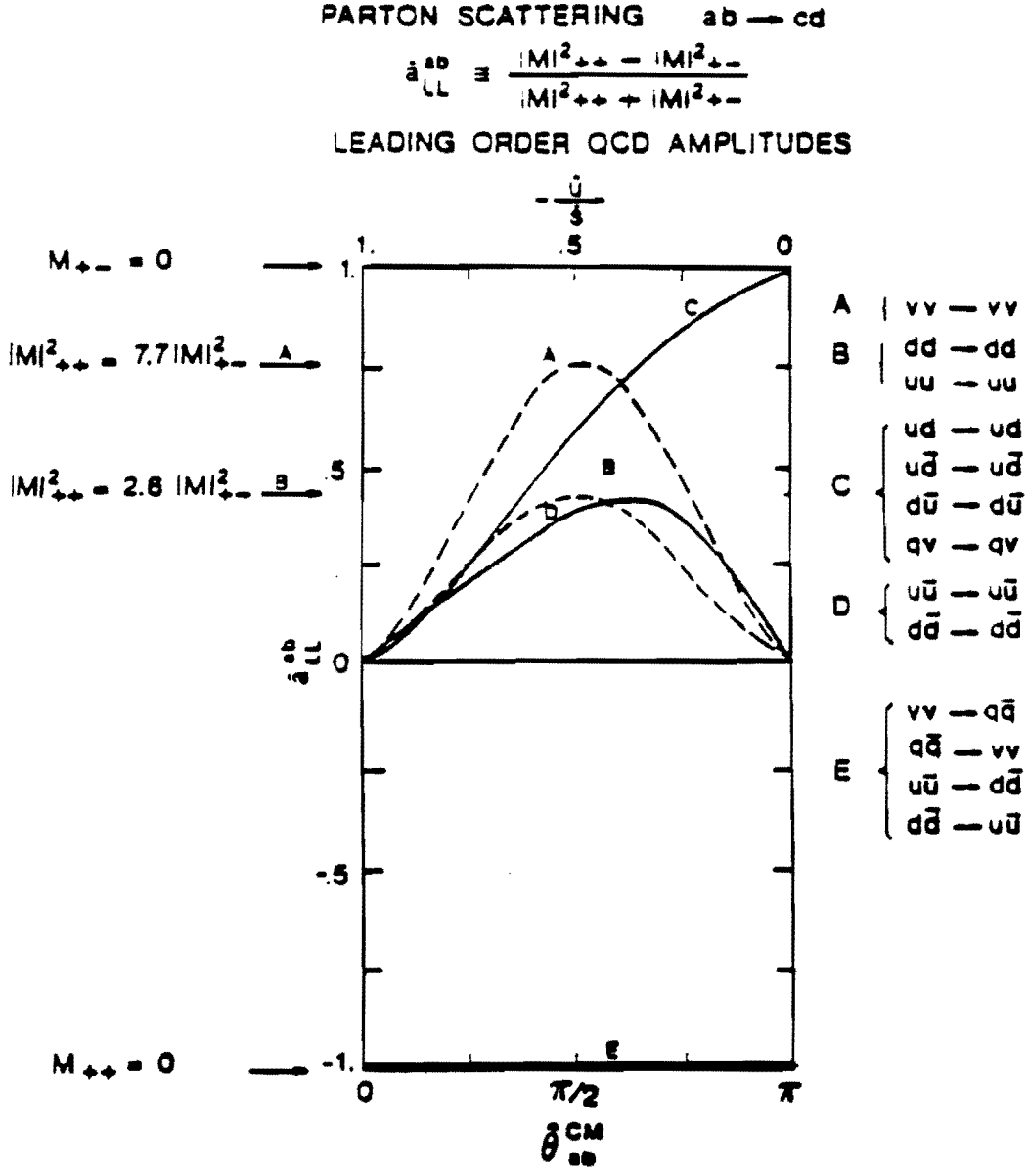

The basic QCD asymmetry $\hat{a}_{LL}^{ij}$ for different classes of diagrams.

Fig. 2

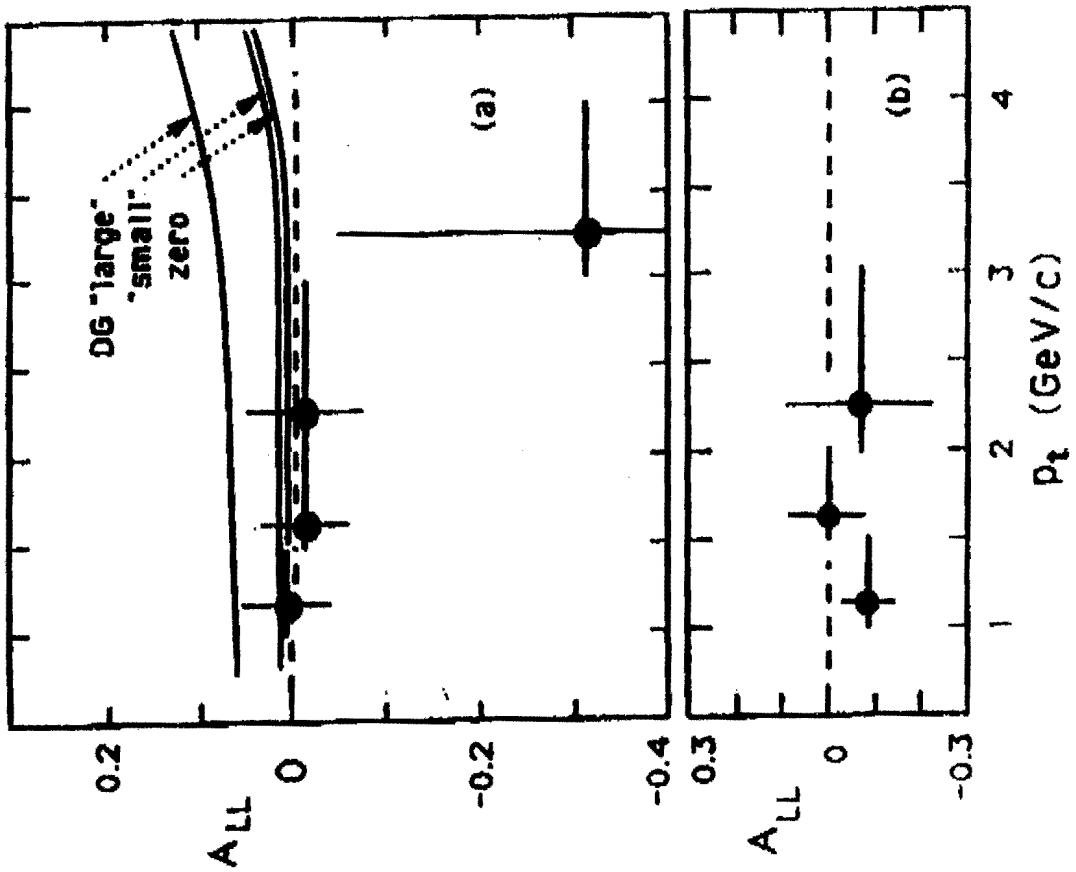

$A_{LL}^{\pi\pi}$ in π^0 production.

Fig. 3

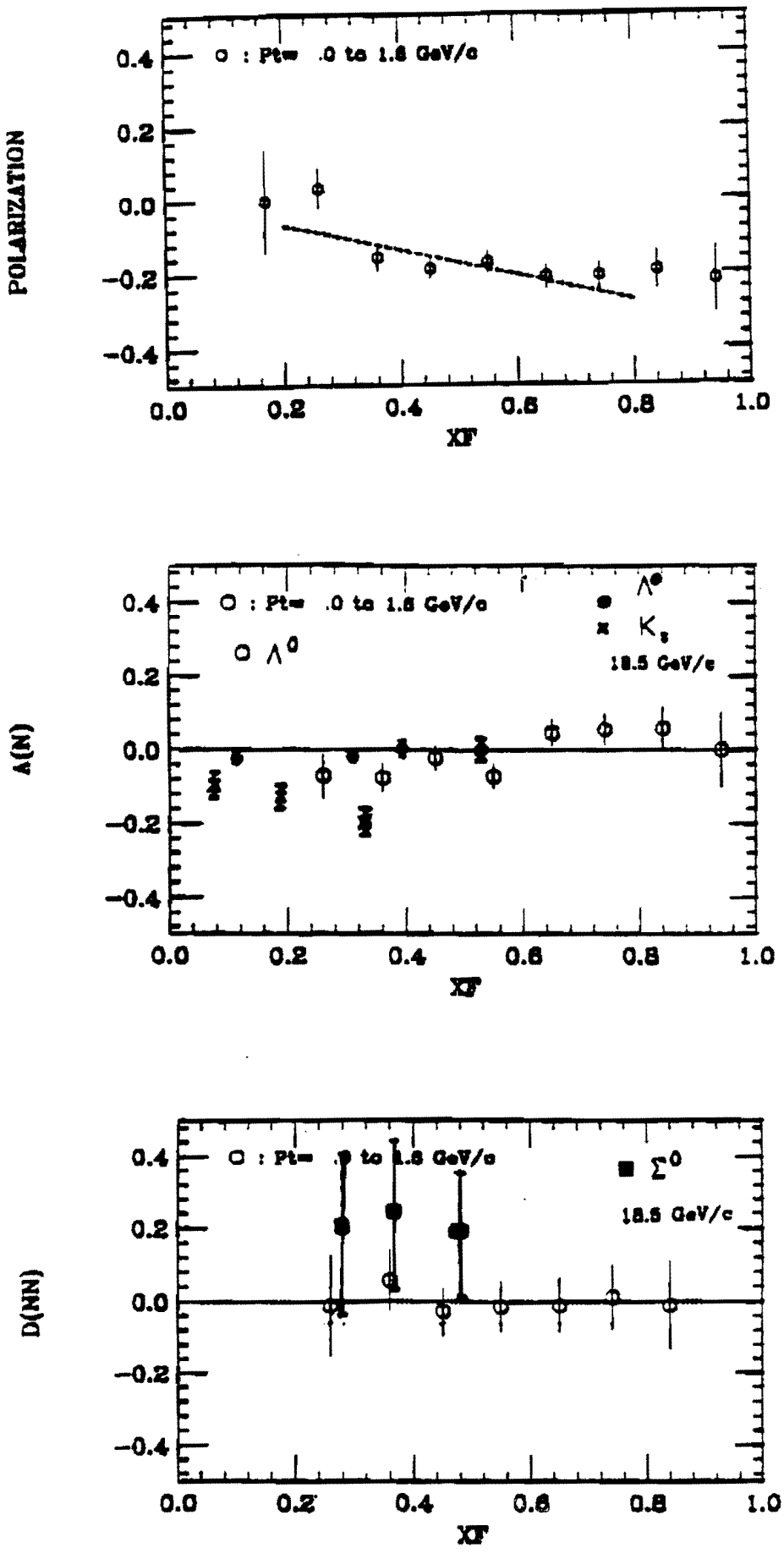

Fig. 4 P_0, A_N, $D_{NN}(= A_{NN}^{\prime\prime})$ for $pp \to \Lambda X$ at 200 GeV/c versus x_F [26].

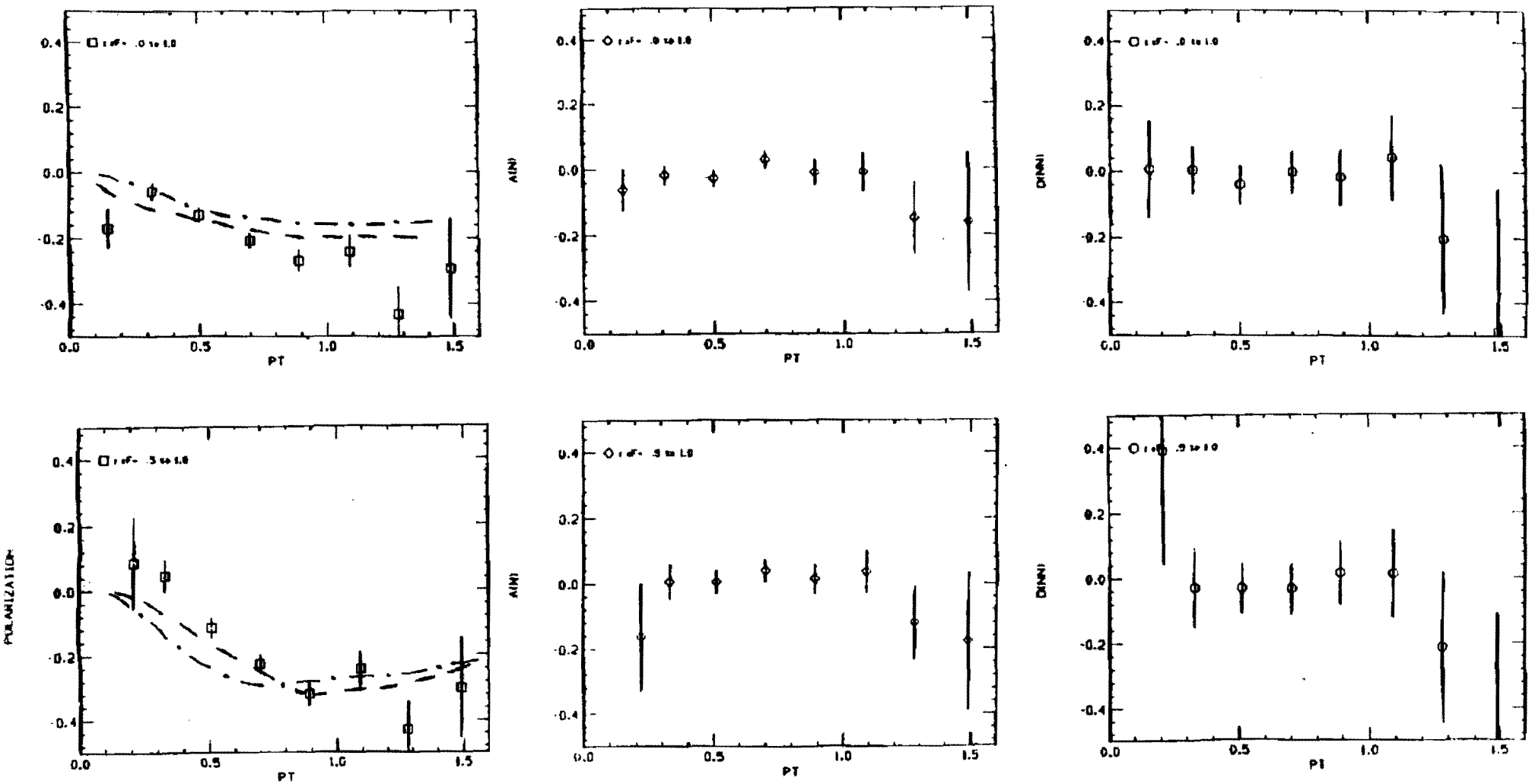

Fig. 5 P_{0}, A_N, D_{NN} for $pp \rightarrow \Lambda X$ at 200 GeV/c versus p_T

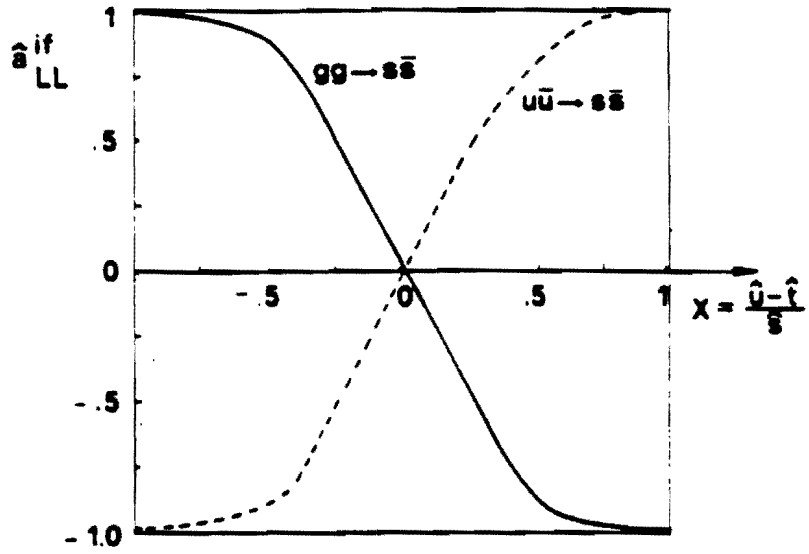

The $\hat{a}_{LL}^{if}$ elementary asymmetry for processes $gg \to s\bar{s}$, $u\bar{u} \to s\bar{s}$.

Fig. 6

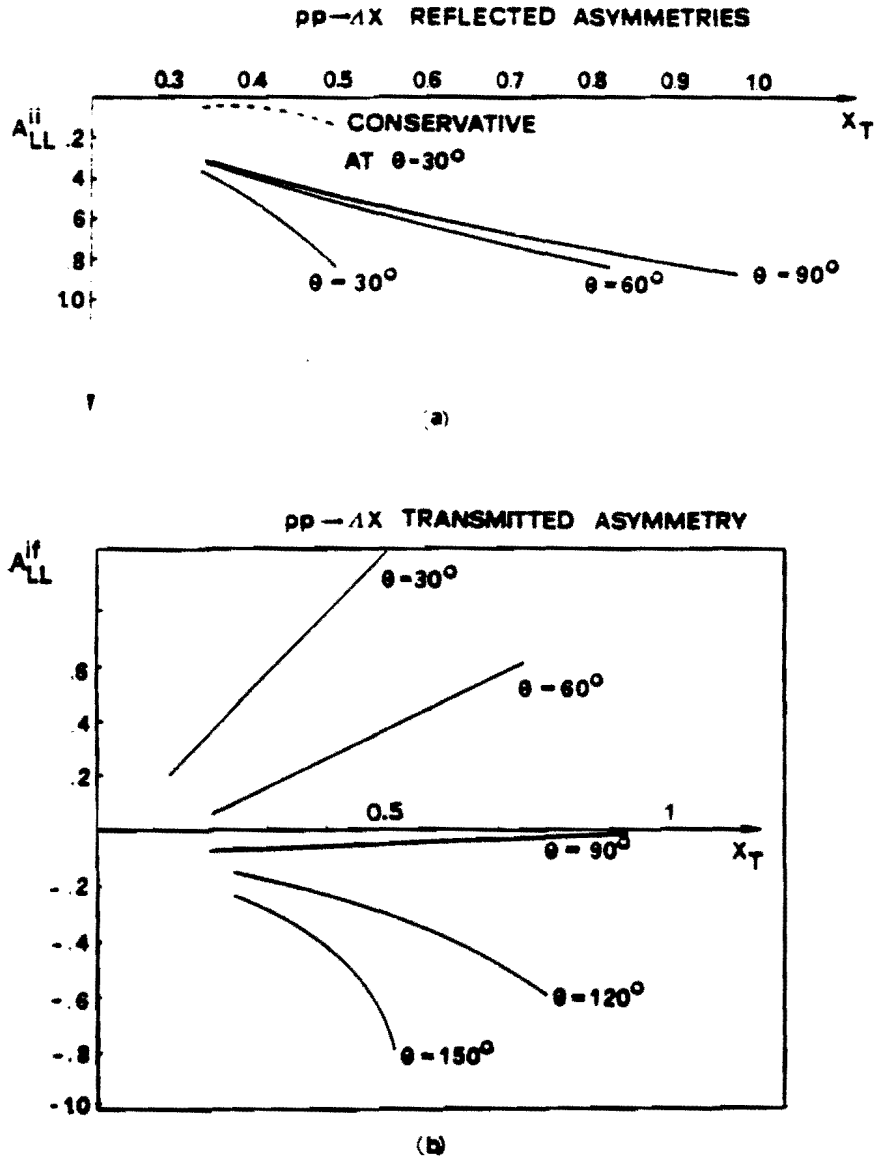

Fig. 7 **Predictions of [12] for helicity asymmetries in $pp \to \Lambda X$.**

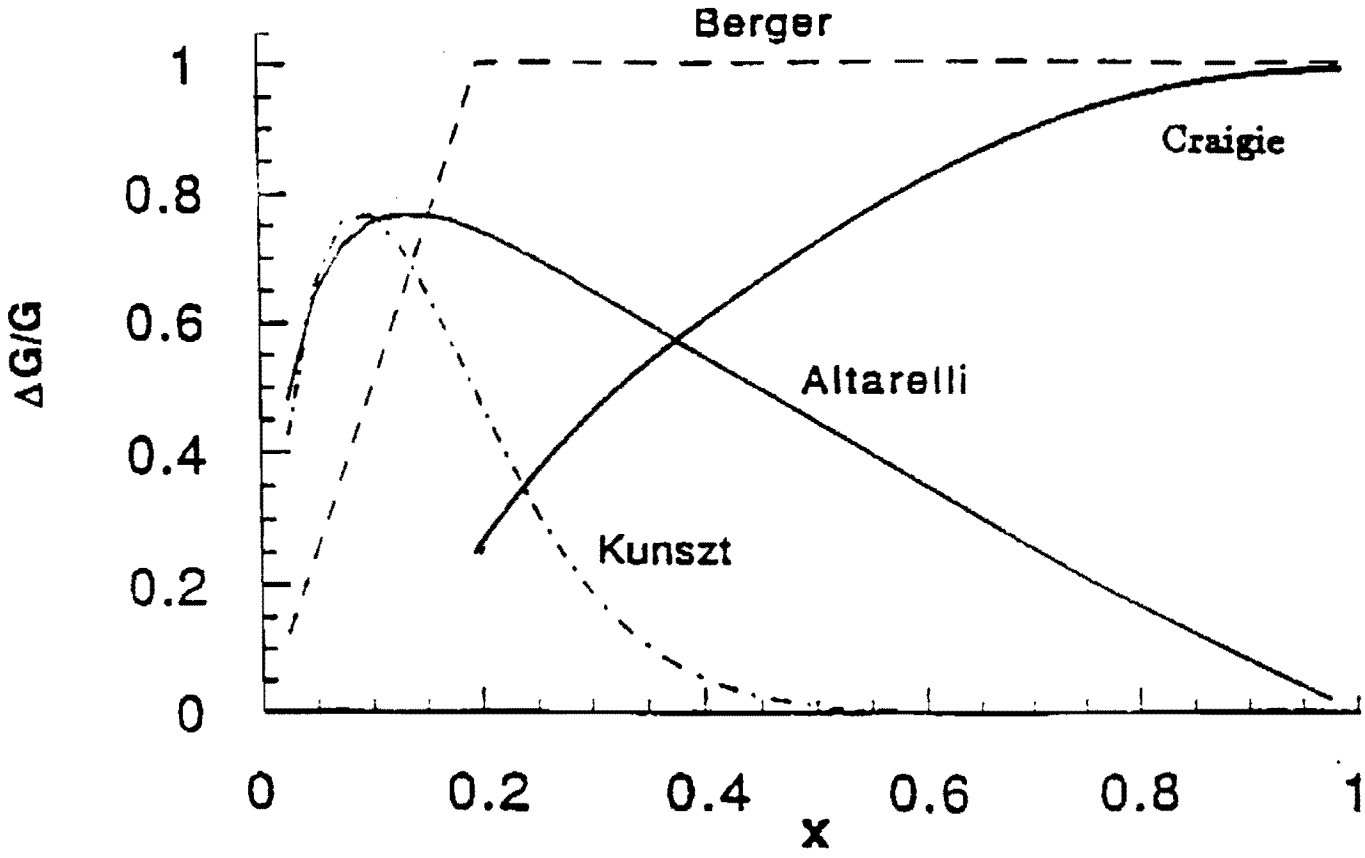

Assumptions of $\Delta G/G(x)$

Fig. 8

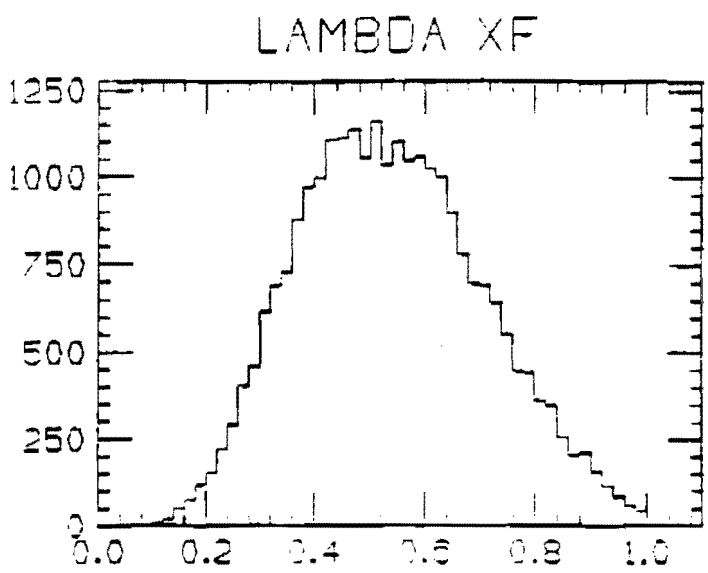

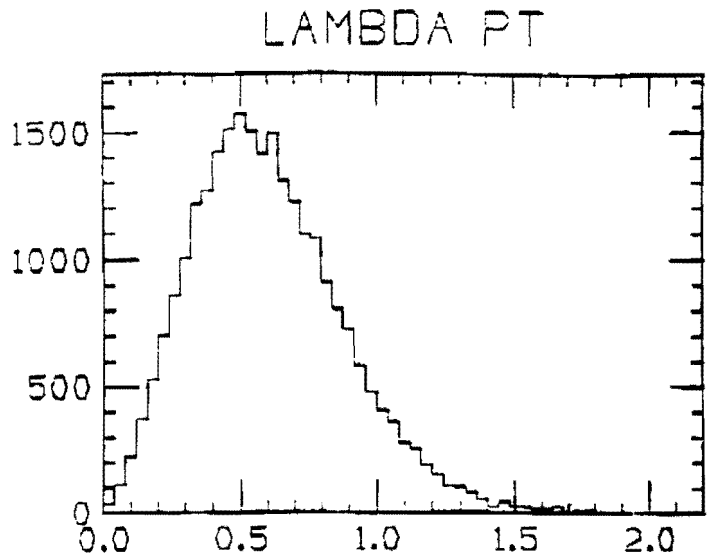

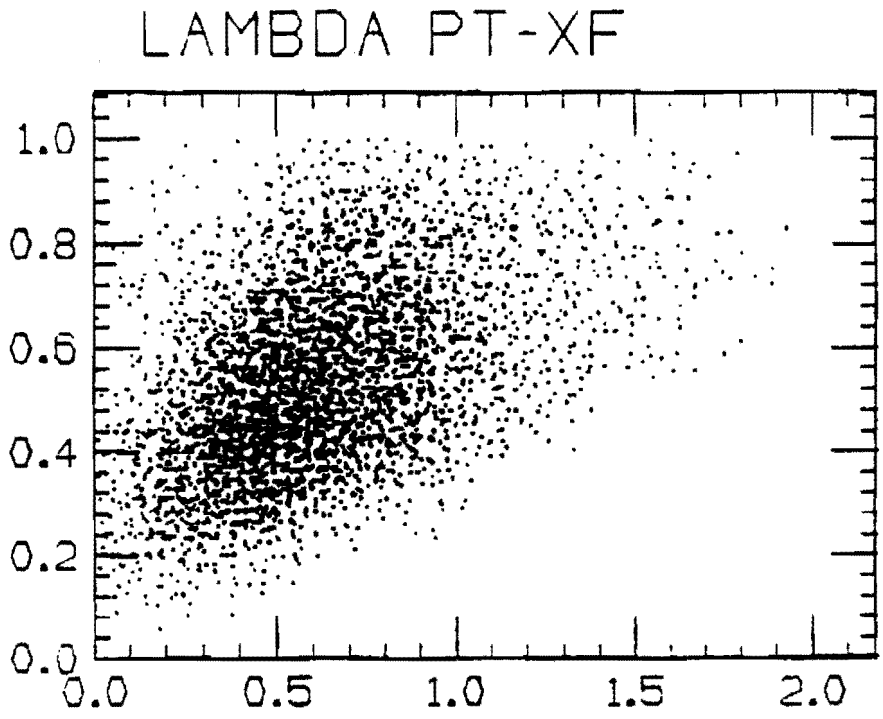

Fig. 9

The E704 experimental phase space for $pp \rightarrow \Lambda X$.

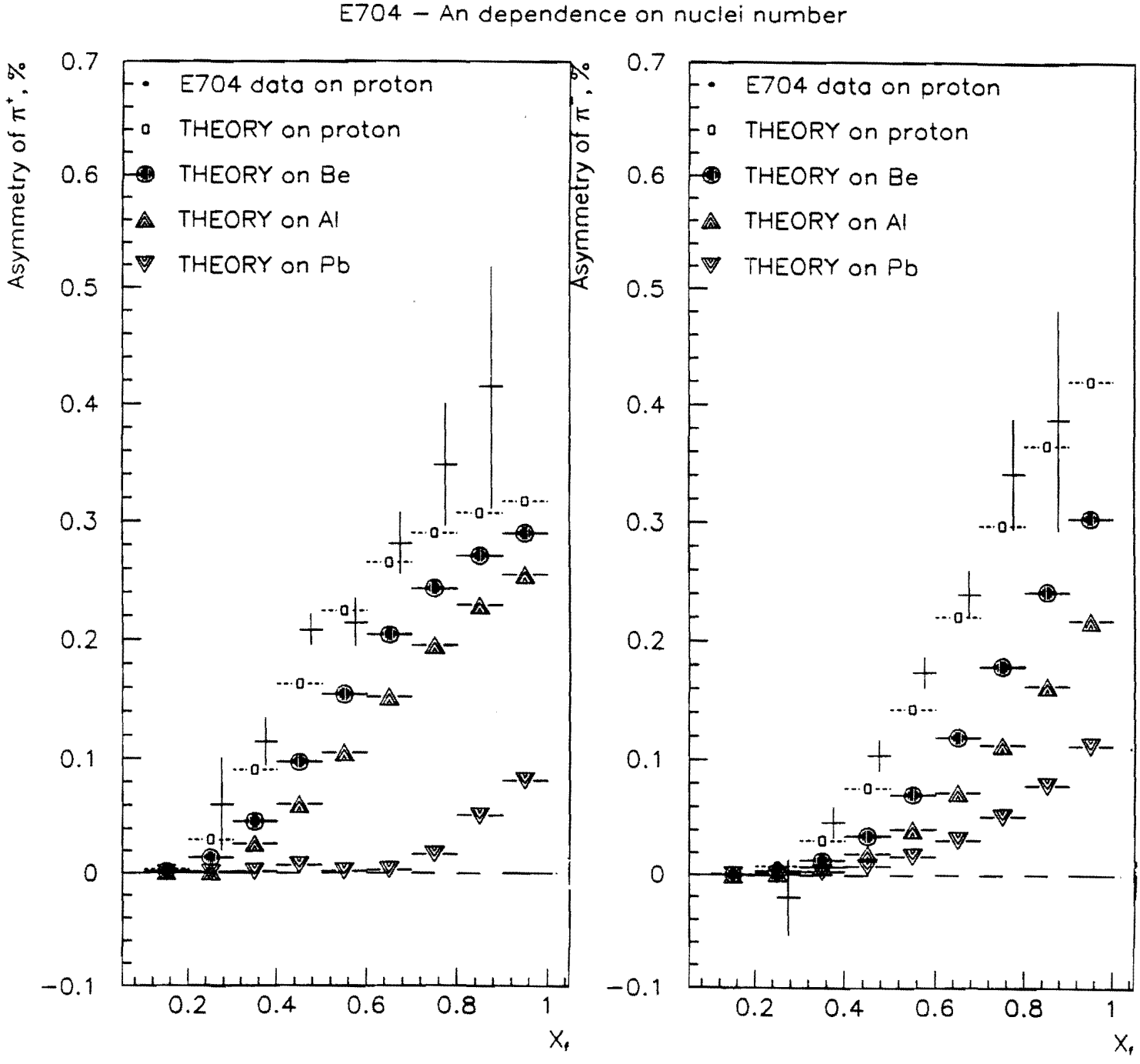
E704 – An dependence on nuclei number
Asymmetry of π^+, %
Asymmetry of π^-, %
E704 data on proton
THEORY on proton
THEORY on Be
THEORY on Al
THEORY on Pb
0.7
0.6
0.5
0.4
0.3
0.2
0.1
0
−0.1
0.2
0.4
0.6
0.8
1
X_f

Fig. 10

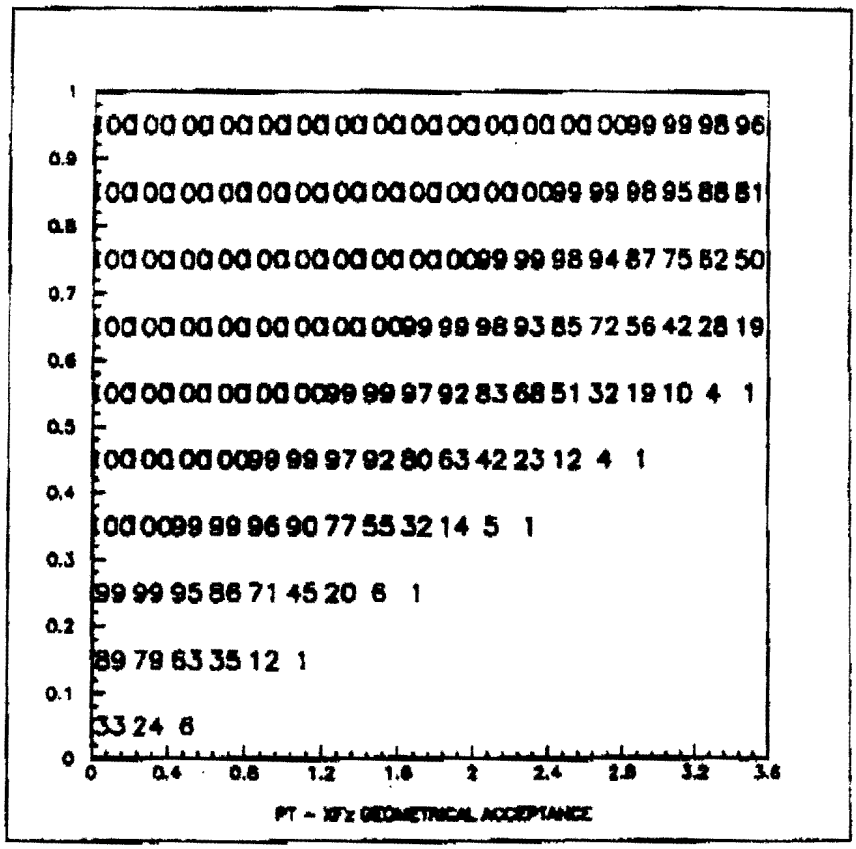

a) Gemetrical acceptance

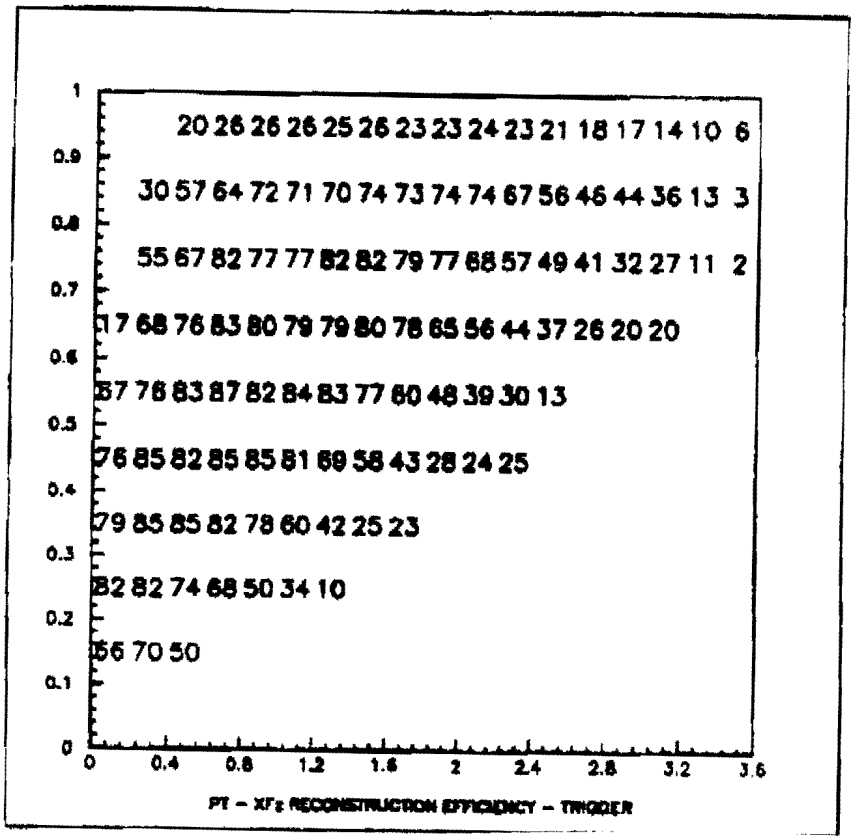

b) Reconstruction efficiency

Fig. 11

for $pp \to \Lambda X$.

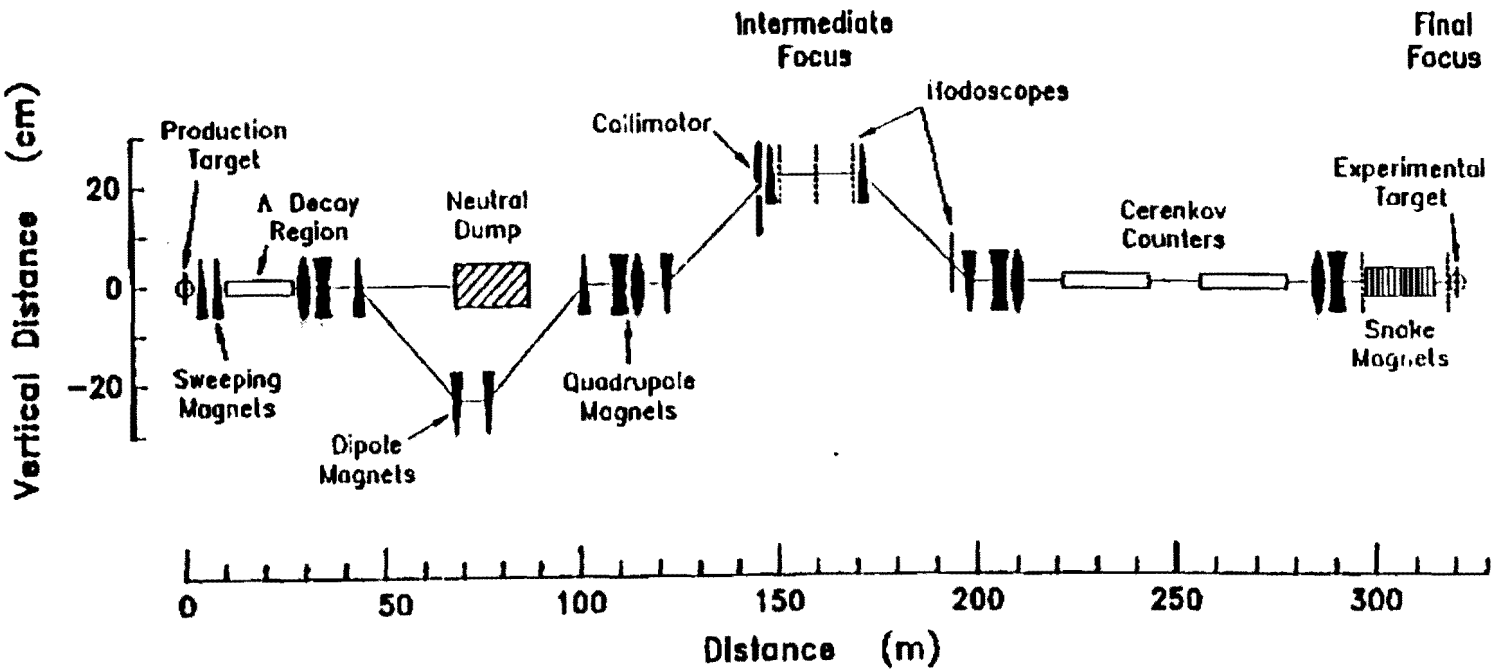

Fig. 12 Layout of elements along the MP polarized beam line. Shown here is a side view of the production target, neutral particle dump, adjustable collimator, beam-tagging region, snake magnets, Čerenkov counters, and experimental target. Note the difference in scale between the horizontal and vertical axes.

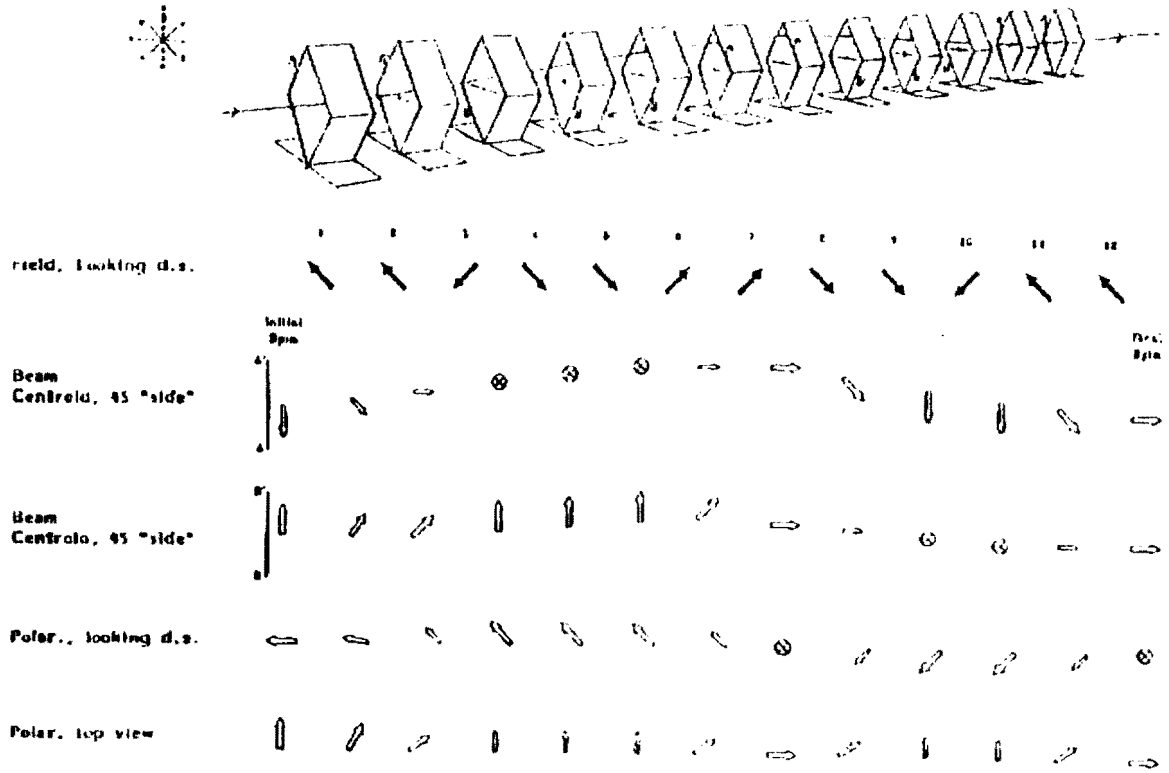

Fig. 13 The type II solution as actually implemented in the Fermilab polarized beam. The overall rotation is π/2 around the vertical axis. We have not used the continuously variable feature. Some of the magnets requiring higher strength are physically made of two magnets and so 12 magnets appear in this diagram.

a) The orbit and field directions.
b) The field directions looking downstream.
c) The spin direction looking from below on the right.
d) The spin direction looking from above on the right.
e) The spin after each magnet, looking downstream.

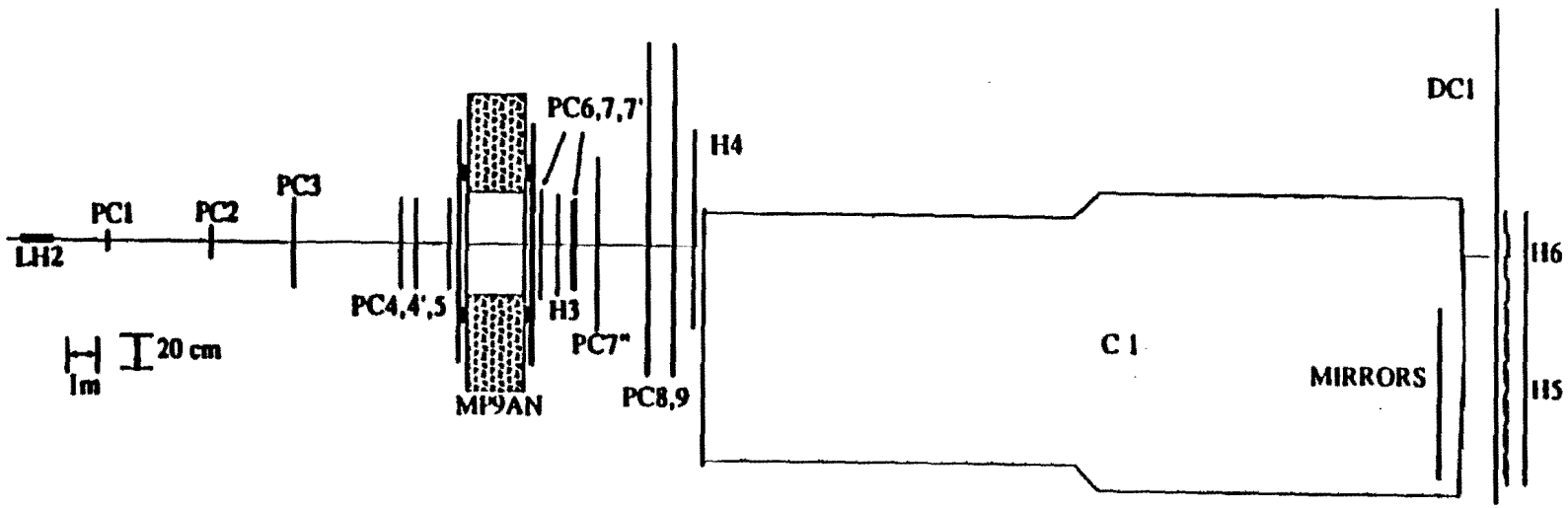

Fig. 14 Essential components of the E704 Forward Spectrometer: the liquid Hydrogen target LH2, tracking chambers (PC's and DC1), trigger scintillation hodoscopes (H's), Cherenkov threshold counter, and diapole analyzing magnet (MP9AN).

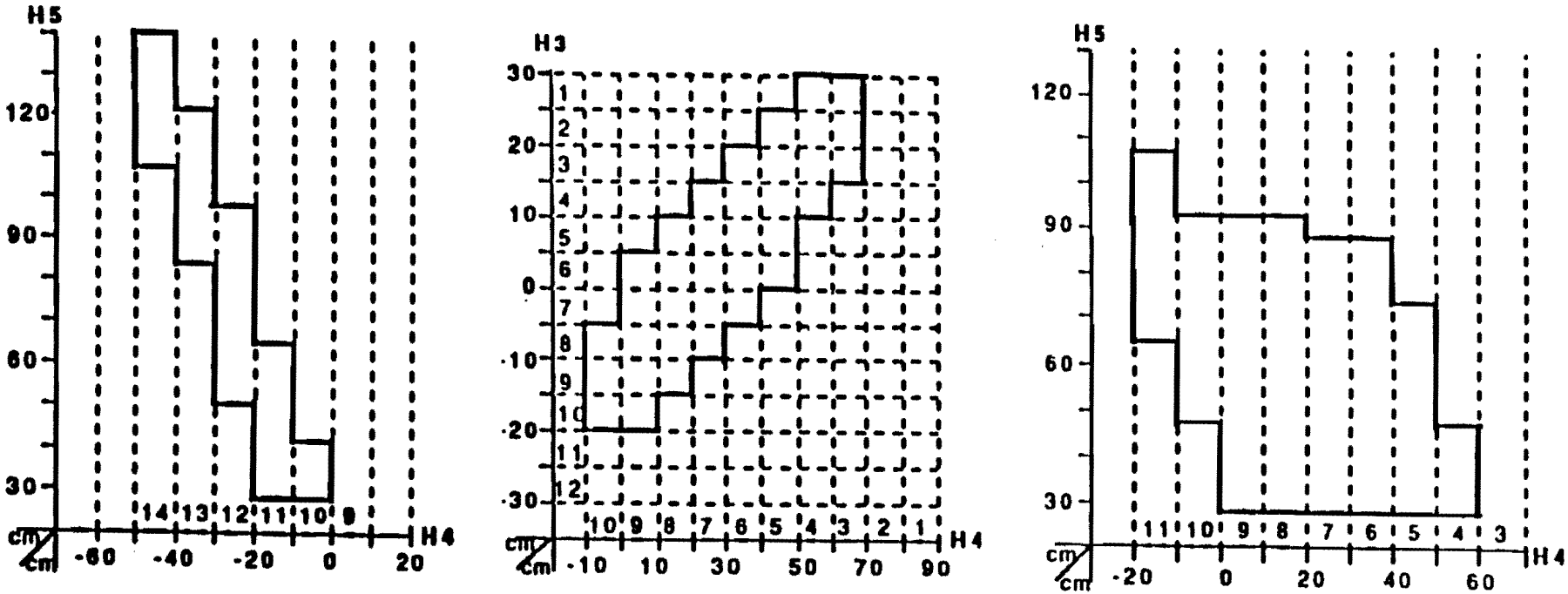

Fig. 15 *(a) Stiff-Proton Correlation:* The x-position of the proton track at the H4 plane is strongly correlated to that at H5 plane. *(b) Soft-Pion Correlation:* Similar but less well-defined is observed for x-positions of the π^- track at H3 and H4. *(c) Proton-Pion Correlation:* Correlation between x-posion of the proton track at H5 to that of the pion's at H4.

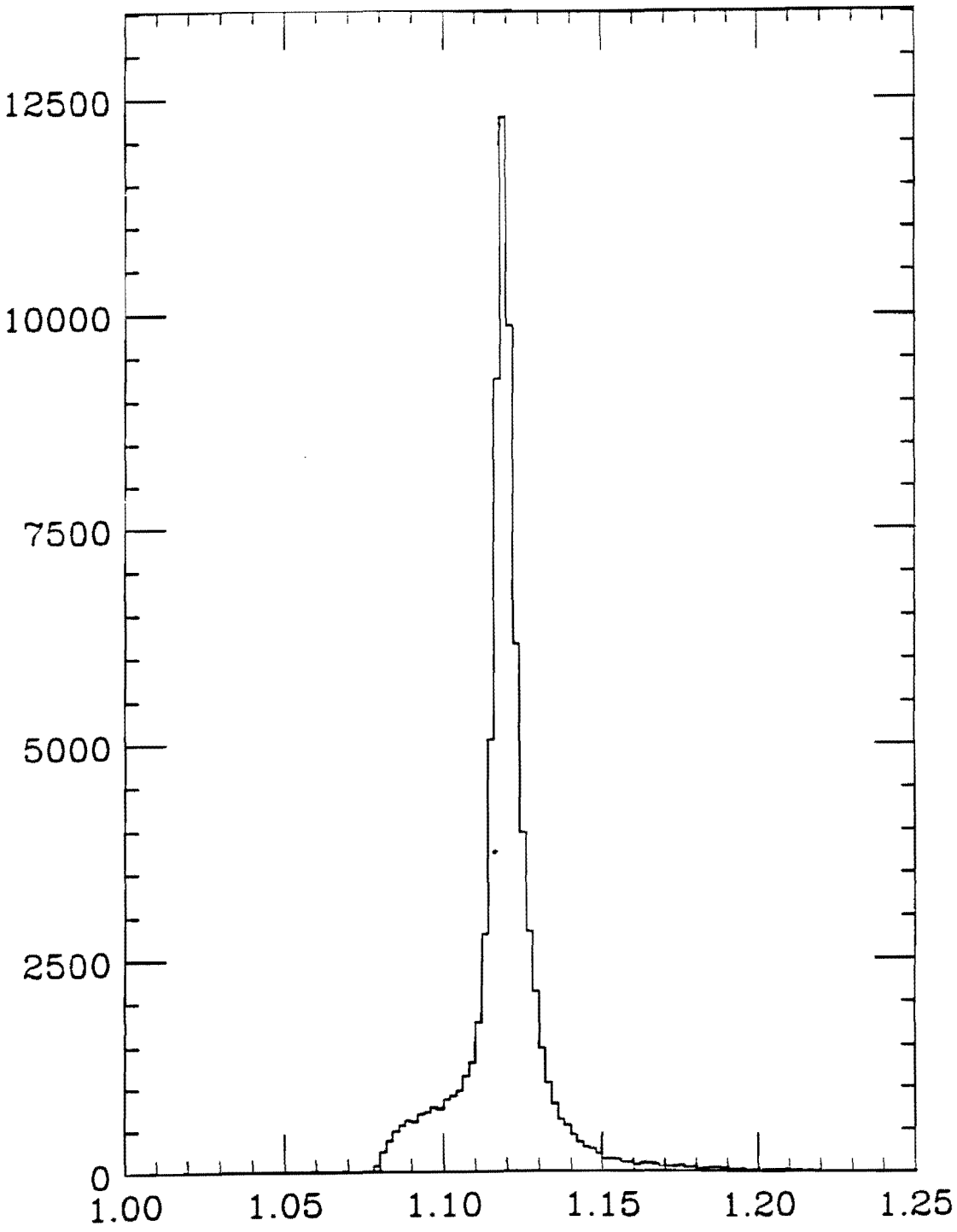

Fig. 16 Proton–pion invariant mass after selection cuts

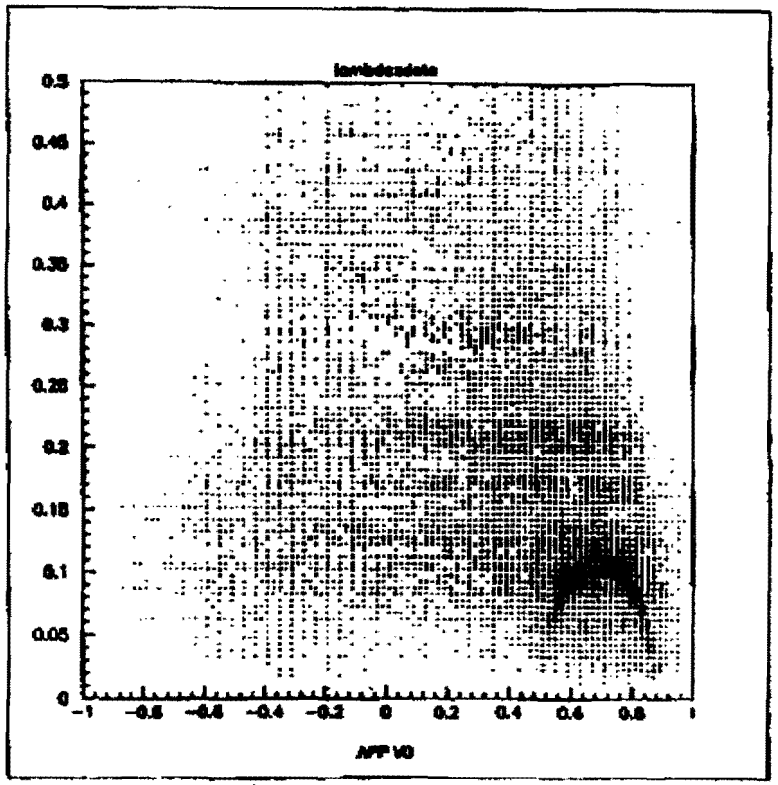

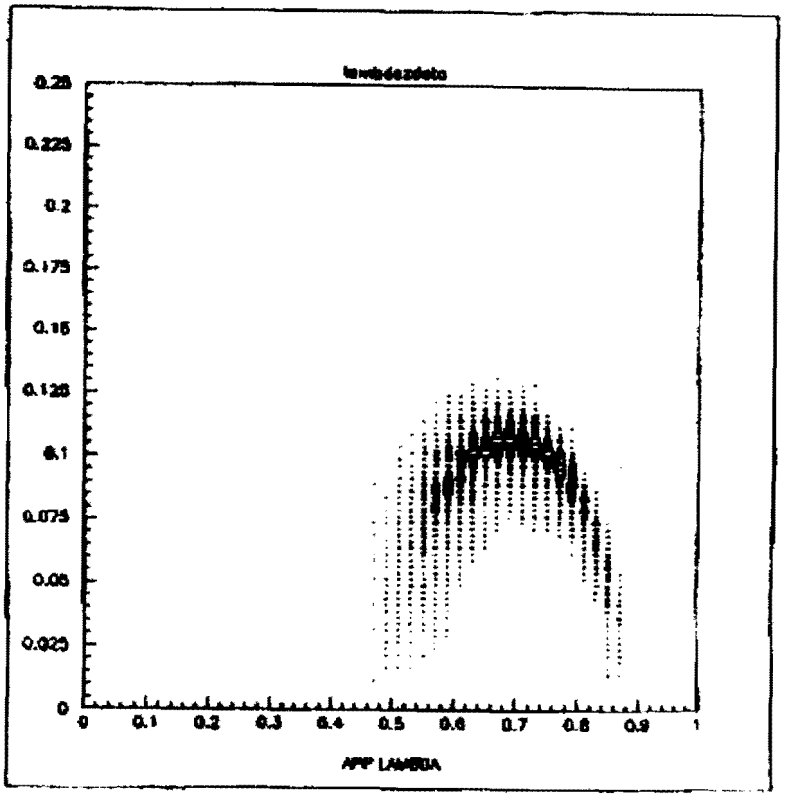

Fig. 17

The V^0 decay phase space $\alpha\ q_T$.

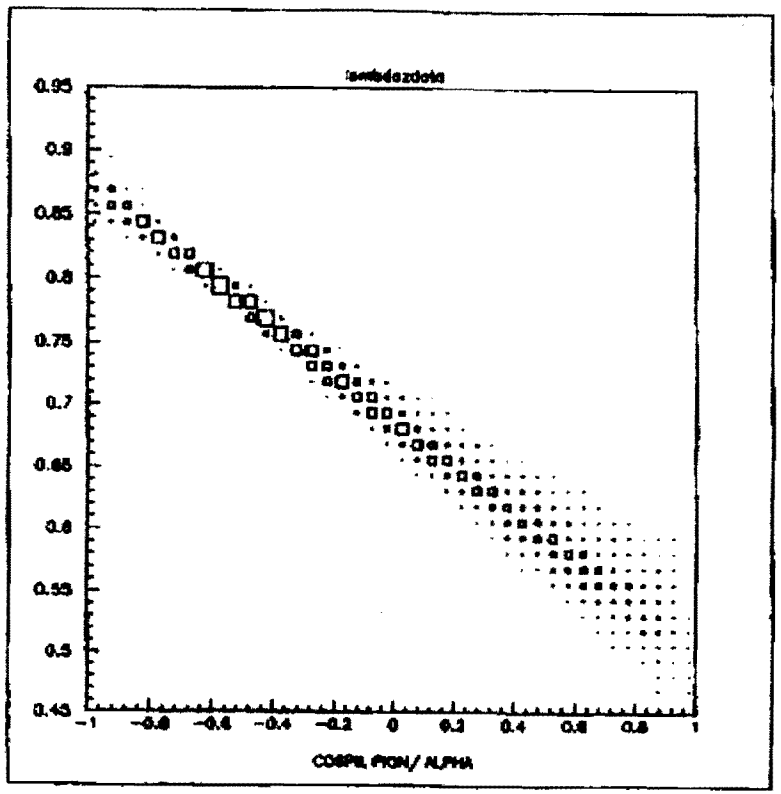

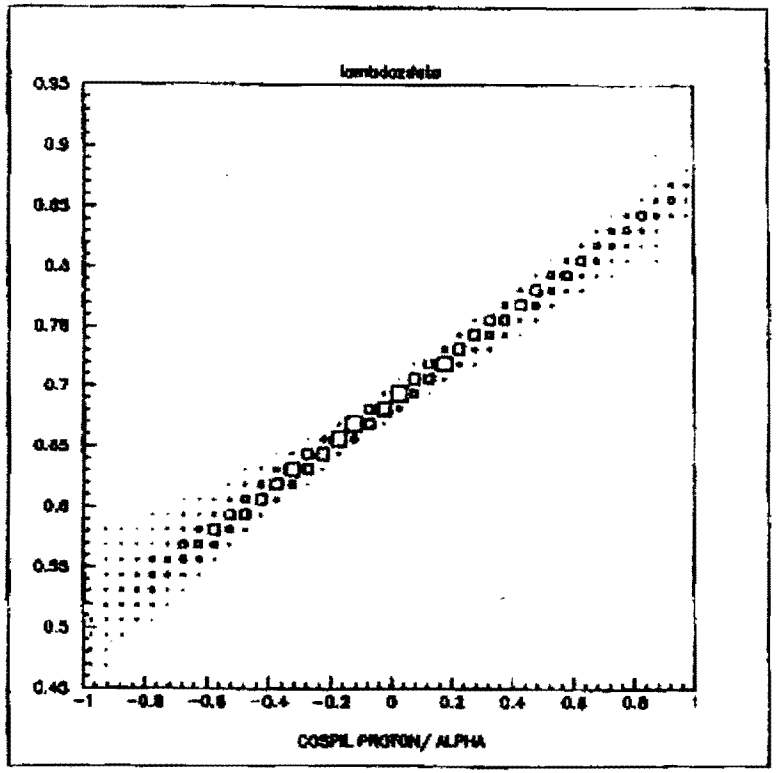

Fig. 18

The correlation between α and π or γ decay angles.

Plane	Type	Chamber	Wire spacing in cm	No. of wires	Offset in cm	Z-Position in cm	Chamber Type
1	X	PC1	0.10	96	0.22	250.2	RMH
2	Y	PC1	0.10	96	0.01	249.2	RMH
3	U	PC1	0.10	96	0.27	253.7	RMH
4	V	PC1	0.10	96	-0.21	245.7	RMH
5	X	PC2	0.10	192	0.01	593.8	RMH
6	Y	PC2	0.10	192	0.06	592.8	RMH
7	U	PC2	0.10	192	0.11	597.3	RMH
8	V	PC2	0.10	192	-0.01	589.3	RMH
9	X	PC3	0.20	128	-0.01	850.2	PCOSIII
10	Y	PC3	0.20	128	0.06	850.2	PCOSIII
11	U	PC3	0.20	240	-1.01	850.2	PCOSIII
12	V	PC3	0.20	240	1.11	850.2	PCOSIII
13	X	PC4	0.20	256	-0.14	1176.0	PCOSIII
14	Y	PC4	0.20	128	-0.14	1176.0	PCOSIII
15	U	PC4	0.20	304	-1.17	1176.0	PCOSIII
16	V	PC4	0.20	304	1.29	1176.0	PCOSIII
17	X	PC4'	0.20	256	-0.09	1246.5	RMH
18	Y	PC4'	0.20	192	-6.25	1244.5	RMH
19	X	PC5	0.20	256	0.02	1358.8	RMH
20	Y	PC5	0.20	256	0.20	1356.4	RMH
21	U	PC5	0.20	256	0.15	1364.2	RMH
22	V	PC5	0.20	256	0.10	1351.0	RMH
23	X	PC6	0.20	320	-0.23	1655.9	RMH
24	Y	PC6	0.20	320	-0.01	1653.5	RMH
25	U	PC6	0.20	320	-0.25	1661.3	RMH
26	V	PC6	0.20	320	0.21	1648.1	RMH
27	X	PC7	0.20	320	-0.08	1746.9	RMH
28	Y	PC7	0.20	320	0.01	1744.5	RMH
29	X	PC7'	0.20	320	-0.13	1761.9	RMH
30	Y	PC7'	0.20	320	0.00	1759.4	RMH
31	V	PC7"	0.20	704	6.14	1839.0	RMH
32	X	PC8	0.20	0	0.00	1967.7	PCOSIII
33	X'	PC8	0.20	1024	19.68	1975.3	PCOSIII
34	U	PC8	0.20	0	0.00	1970.2	PCOSIII
35	V	PC8	0.20	1024	-16.40	1972.8	PCOSIII
36	X	PC9	0.20	1024	19.85	2071.5	PCOSIII
37	X'	PC9	0.20	1024	19.73	2079.1	PCOSIII
38	U	PC9	0.20	1024	18.27	2074.0	PCOSIII
39	V	PC9	0.20	1024	-16.39	2076.6	PCOSIII
40	X	PC15	0.20	384	-80.00	4690.0	RMH
41	Y	PC15	0.20	448	0.00	4690.0	RMH
42	X	DC1	1.96	160	-0.21	4700.0	Drift Chamber
43	X'	DC1	1.96	160	0.72	4705.0	Drift Chamber
44	U	DC1	1.86	176	2.75	4700.0	Drift Chamber
45	V	DC1	1.86	176	1.54	4700.0	Drift Chamber
46	X	BI1	0.10	96	-0.05	-2350.0	RMH
47	Y	BI1	0.10	96	-0.08	-2350.0	RMH
48	X	BI2	0.10	96	0.07	-516.0	RMH
49	Y	BI2	0.10	96	0.07	-516.0	RMH
50	X	BI3	0.10	96	0.04	-197.8	RMH
51	Y	BI3	0.10	96	0.05	-197.8	RMH

TABLE 1: A summary of specifications and locations of Multi-Wire Proportional Chambers used in the Fermilab E704 forward spectrometer.

Detector	Size (in cm)	Position (x,y,z)	Description
LH2	3,3,100	0,0,0	Cylindical Liquid Hydrogen Target
MP9AN	228.162.282	0.0.1500	1.4 Tesla Dipole Magnet
Gap	42,54,282	0,0,1500	Magnet's Gap
H3	50,50,1	0,0,1635	Hodoscope, 10 segments
H4	120.60.1	10.0,2130	Hodoscope, 12 segments
H5	116.100.1	86.0,4725	Hodoscope, 12 segments
H6	56,100,1	-7,0,4725	Hodoscope, 4 segments
C1	102.102,2400	-78.8,-8.7,4550.	Cherenkov Threshold Counter

TABLE 2: Description of the detectors of the forward spectrometer and their location.